

Accepted Manuscript

Design, Synthesis, and Anticancer Evaluation of Long-chain Alkoxylated Mono-carbonyl Analogues of Curcumin

Qiaoyou Weng, Lili Fu, Gaozhi Chen, Junguo Hui, Jingjing Song, Jianpeng Feng, Dengjian Shi, Jiansong Ji, Professor, Guang Liang, Ph.D, Professor Director



PII: S0223-5234(15)30220-8

DOI: [10.1016/j.ejmech.2015.08.036](https://doi.org/10.1016/j.ejmech.2015.08.036)

Reference: EJMECH 8072

To appear in: *European Journal of Medicinal Chemistry*

Received Date: 16 April 2015

Revised Date: 12 August 2015

Accepted Date: 15 August 2015

Please cite this article as: Q. Weng, L. Fu, G. Chen, J. Hui, J. Song, J. Feng, D. Shi, J. Ji, G. Liang, Design, Synthesis, and Anticancer Evaluation of Long-chain Alkoxylated Mono-carbonyl Analogues of Curcumin, *European Journal of Medicinal Chemistry* (2015), doi: 10.1016/j.ejmech.2015.08.036.

This is a PDF file of an unedited manuscript that has been accepted for publication. As a service to our customers we are providing this early version of the manuscript. The manuscript will undergo copyediting, typesetting, and review of the resulting proof before it is published in its final form. Please note that during the production process errors may be discovered which could affect the content, and all legal disclaimers that apply to the journal pertain.

Design, Synthesis, and Anticancer Evaluation of Long-chain Alkoxyated Mono-carbonyl Analogues of Curcumin

Qiaoyou Weng^{1,2#}, Lili Fu^{1#}, Gaozhi Chen¹, Junguo Hui², Jingjing Song², Jianpeng Feng¹, Dengjian Shi¹, Jiansong Ji^{2*}, Guang Liang^{1*}

1. Chemical Biology Research Center, School of Pharmaceutical Sciences, Wenzhou Medical University, Wenzhou, Zhejiang 325035, China
2. Department of Interventional Radiology, The Fifth Affiliated Hospital of Wenzhou Medical University, Lishui, Zhejiang 323000, China

#These Authors contributed equally to this work

* Corresponding authors:

Guang Liang, Ph.D, Professor

Director, Chemical Biology Research Center

School of Pharmaceutical Sciences, Wenzhou Medical University

Tel: (+86)-577-86699396; Fax: (+86)-577-86699396

E-mail: wzmliangguang@163.com

and

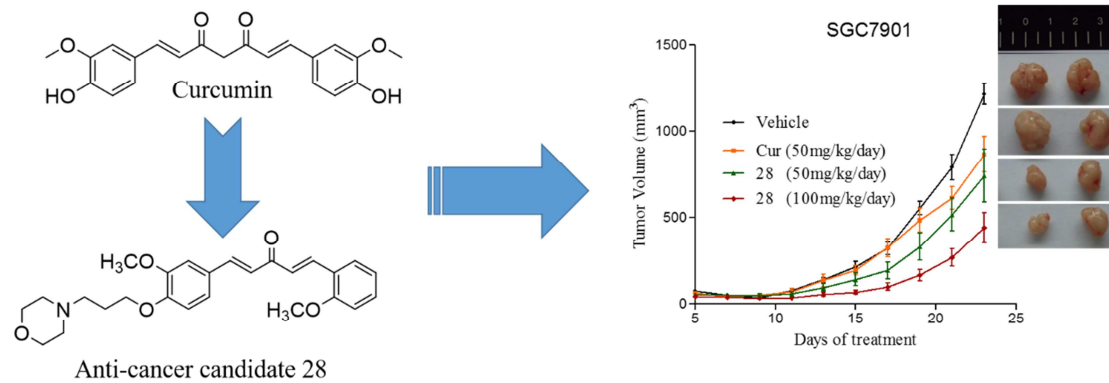
Jiansong Ji, Professor

Department of Interventional Radiology, the Fifth Affiliated Hospital of Wenzhou Medical University

E-mail: jjstcty@sina.com

Graphical abstract

Novel curcumin analogues were synthesized and revealed as potent anti-cancer candidate.



Keywords: anticancer drug, gastric cancer, drug design, MACs, apoptosis

Design, Synthesis, and Anticancer Evaluation of Long-chain Alkoxyated Mono-carbonyl Analogues of Curcumin

Qiaoyou Weng^{1,2#}, Lili Fu^{1#}, Gaozhi Chen¹, Junguo Hui², Jingjing Song², Jianpeng Feng¹, Dengjian Shi¹, Yuepiao Cai¹, Jiansong Ji^{2*}, Guang Liang^{1*}

1. Chemical Biology Research Center, School of Pharmaceutical Sciences, Wenzhou Medical University, Wenzhou, Zhejiang 325035, China
2. Department of Interventional Radiology, The Fifth Affiliated Hospital of Wenzhou Medical University, Lishui, Zhejiang 323000, China

#These Authors contributed equally to this work

* Corresponding authors:

Guang Liang, Ph.D, Professor

Director, Chemical Biology Research Center

School of Pharmaceutical Sciences, Wenzhou Medical University

Tel: (+86)-577-86699396; Fax: (+86)-577-86699396

E-mail: wzmliangguang@163.com

and

Jiansong Ji, Professor

Department of Interventional Radiology, the Fifth Affiliated Hospital of Wenzhou Medical University

E-mail: jjstcty@sina.com

Abstract: Curcumin is a nontoxic phenolic compound that modulates the activity of several cellular targets that have been linked with cancers and other chronic diseases. However, the efficacy of curcumin in the clinic has been limited by its poor bioavailability and rapid metabolism *in vivo*. We have previously reported the design and discovery of series of 5-carbon linker-containing mono-carbonyl analogues of curcumin (MACs) as anti-cancer agents. In continuation of our ongoing research, we designed and synthesized 37 novel long-chain alkoxyated MACs for anti-cancer evaluation here. The MTS assay was used to determine the cytotoxicity of compounds in gastrointestinal cancer cells. Compounds **5**, **28**, and **29** showed strongest inhibition against gastric cancer cell proliferation and were subjected to further analysis. The effects of **5**, **28**, and **29** on cell apoptosis were measured by flow cytometry. Expression levels of Bcl-2, cleaved poly ADP-ribose polymerase (PARP), and pro-caspase-3 were detected by western blotting. Compounds **5**, **28**, and **29** induced apoptosis in human gastric carcinoma cells, increased PARP cleavage, and decreased expression of Bcl-2 and cleavage of PARP protein. We then showed that compound **28**, **which** possessed the strongest activity among the test compounds *in vitro*, exhibited significant tumour inhibition in an SGC-7901-driven xenograft mouse model. Taken together, the novel compound **28** could be further explored as an effective anticancer agent for the treatment of human gastric cancer.

Keywords: anticancer drug, gastric cancer, drug design, MACs, apoptosis.

1. Introduction

Despite a sharp decline in its incidence during the second half of the 20th century, gastric cancer remains the fourth most frequently diagnosed type of cancer and the second most common cause of cancer-related deaths worldwide[1-3], with 988,000 new cases and 736,000 deaths per year[4-6]. Almost two-thirds of gastric cancer cases occur in developing countries, and 42% of cases occur in China[7]. Prognosis of gastric cancer is generally poor with a 5-year relative survival below 30% in most countries[8]. Surgery and chemotherapy are the most popular therapy for gastric cancer [9, 10]. Surgical resection is the primary treatment for gastric cancer and it can cure the patients with early-stage cancer. *Yung-Jue Bang* and colleagues reported a 5-year survival rate of 36% in patients with operable disease who received perioperative chemotherapy. However, the 5-year survival rate for advanced or metastatic gastric cancer patients is around 5–20%[11]. Gastric cancer at an early stage may be clinically silent, and in most countries, patients are diagnosed at an advanced stage when the tumor is unresectable or metastatic. For these patients, as well as disease recurrence after initial surgical treatment, systemic chemotherapy is the main treatment option even though it prolongs survival without compromising quality of life[12].

Although a large number of chemotherapy regimens have been tested in randomized clinical studies, there is still no internationally accepted standard for the gastric cancer treatment. Existing chemotherapeutic formulations containing fluoropyrimidine and cisplatin do not have ideal curative effects and have many undesirable side effects [13-15]. Therefore, most gastric cancer patients who diagnosed with inoperable advanced or metastatic cancer require palliative care. Development of pharmacologically effective agents with acceptable toxicity profiles has become an urgent demand.

Numerous types of anti-cancer compounds exist in edible and medicinal plants, and chemical and pharmacological investigations of such compounds are in progress [16-18]. The phenolic diarylheptanoid curcumin is the major pigment in turmeric [19] and has been found to inhibit multiple cancer types via its effect on several biological pathways involved in mutagenesis, cell cycle regulation, oncogene expression, apoptosis, tumorigenesis, and metastasis [20]. These findings regarding the molecular mechanisms of curcumin shows that it worth to further consideration as a treatment for cancer. However, rapid plasma clearance and low bioavailability significantly limit the therapeutic application of curcumin [21]. Due to the metabolic instability, the β -diketone moiety of curcumin was displaced with a single carbonyl group in our previous study, and a series of mono-carbonyl analogues of curcumin (MCACs) were synthesized and evaluated the pharmacokinetics and cytotoxicity. Some MCACs exhibited enhanced stability *in vitro* and greatly improved pharmacokinetic profiles *in vivo*. Some MCACs exhibited higher cytotoxic than the lead compound curcumin. The structure-activity relationship analysis in our previous work showed that MCACs with electron-withdrawing substitutions or weak electron-donating substitutions increased cytotoxicity (Figure 1)[22]. Furthermore, due to the frequently presence of a long-chain alkoxy group in several anticancer drugs, such as foretinib, gefitinib, cediranib, and SKI-606, we

proposed that the MCACs with long-chain alkoxy groups might have more increased pharmacological activity in comparison with other MCACs. Thus, in the present study, we designed a series of long-chain alkoxyated mono-carbonyl analogues of curcumin and tested their anti-tumour activity *in vivo* and *in vitro*.

Please insert Figure 1

2. Results and Discussion

2.1 Chemistry

The common synthetic route and structures of compounds **1–22** are outlined in Figure 2. Intermediate 2 was prepared from hydroxybenzaldehyde and aliphatic dibromoalkanes in 1 step. Intermediate 2 was refluxed with appropriate amines in basic conditions to afford intermediate 3. Compounds **1–22** were prepared by the aldol condensation reaction of cyclic ketones and intermediate 3 with yields of 15.4%–72.9%. For the synthesis of compounds **23–37** (Figure 3), intermediate 4 was first produced through the aldol condensation reaction of intermediate 3 and acetone in a basic solution. A one-step aldol condensation reaction was used to produce compounds **23–37** (24.3%–76.8%) using substituted benzaldehydes and intermediate 4.

The structures of all compounds were characterized using $^1\text{H-NMR}$ and electrospray ionization mass spectrometry (ESI-MS) and three most active compounds were further characterized by $^{13}\text{C-NMR}$. Before they were used in biological experiments, all synthesized compounds were purified by recrystallization or silica gel column chromatography, and HPLC was used to determine their purity (all >95%).

Please insert Figure 2

Please insert Figure 3

2.2 Inhibitory Activity on Gastrointestinal Carcinoma Cells of All Compounds

The anti-proliferative effects of compounds **1–37** in 4 gastrointestinal carcinoma cell lines (MGC803, SGC7901, CT26, and SW620) were determined by MTS assay (Promega, San Luis Obispo, CA, USA) at a concentration of 10 μM (**Table S1**). Surprisingly, 20 of the test compounds inhibited the growth of the 4 gastrointestinal carcinoma cell lines by more than 50% at a concentration of 10 μM , and the IC_{50} s of these 20 compounds against the MGC803, SGC7901, CT26, and SW620 cell lines were determined (**Table 1**). The 20 tested compounds showed excellent anti-proliferative activity in 4 gastrointestinal carcinoma cell lines ($\text{IC}_{50} = 0.18\text{--}8.46$ μM), with the exceptions of compounds **2** and **9**. One of the most noteworthy results of this experiment was that compounds **5, 16, 18, 28, and 29** inhibited SGC-7901 cells more effectively than the other tested compounds. Further evaluation of the toxicity and physicochemical properties of compounds **5, 16, 18, 28, and 29** were shown in Figure

S1-S5. Compounds **16** and **18** showed poor solubility at 3.63µg/ml and 4.11µg/ml, much lower than that of compounds **5**, **28**, and **29** (21.65µg/ml, 21.23µg/ml, and 113.5µg/ml, respectively). Thus, in consideration of their toxicity, solubility, and activity, compounds **5**, **28**, and **29** were chosen for further studies.

Please insert Table 1

2.3 Induction of Apoptosis by compounds in Vitro

The effects of compounds **5**, **28**, and **29** on SGC-7901 tumour cell apoptosis were tested, curcumin served as a positive control. SGC-7901 tumour cells were treated with various concentrations of the test compounds or vehicle for 30 h. The cells were harvested and stained with Annexin-V and PI, the proportions of apoptotic cells in each group were determined by flow cytometry analysis. Compounds **5** and **28** significantly and dose-dependently increased apoptosis in SGC7901 cells in comparison with the negative control cells (**Figure 4**), while compound **29** did not exhibit this activity. By comparing the pro-apoptotic effects of the test compounds, we found that compound **28** exhibited a superior pro-apoptotic activity and that its effect was dose-dependent. Compound **28** induced apoptosis in approximately 50% of treated SGC7901 cells at a concentration of 10 µM, demonstrating that it was the most effective of the tested compounds in SGC7901 cells.

Please insert Figure 4

2.4 Effects of compounds on apoptosis proteins

To determine the mechanisms underlying the pro-apoptotic activity of the test compounds, we examined the effects of compounds **5**, **28** and **29** on apoptosis-related proteins in SGC7901 cells, using curcumin as a control treatment. SGC7901 cells were treated with various concentrations of compounds **5**, **28**, and **29**. Expression and activation of apoptosis-related signalling molecules (cleaved PARP, Bcl-2, and pro-caspase-3) were determined by immunoblotting (**Figure 5**). The caspase-3 signalling pathway, a pro-oncogenic pathway, plays a key role in regulation of cell functions via regulation of genes involved in cell proliferation [23]. Activation of caspase-3 was indicated by a decrease in the abundance of pro-caspase-3 fragments. As shown in **Figure 5**, caspase-3 activation was observed after exposure to compounds **5**, **28**, and **29**. Bcl-2 family proteins, which have either pro- or anti-apoptotic activities, have been studied intensively for the past decade because of their importance in the regulation of apoptosis, tumorigenesis, and cellular responses to anti-cancer therapy[24]. In the Bcl-2 protein family, anti-apoptotic member Bcl-2 is the active effector and regulator which affect apoptosis induction [25, 26]. Treatment with compounds **5** and **28** significantly decreased Bcl-2 expression. The presence of cleaved PARP is generally considered a marker of apoptosis [27]. Compounds **5** and **28** increased cleaved PARP abundance in SGC7901 cells in a dose-dependent manner, suggesting increased apoptosis 24 hours after treatment with the compounds. In

accordance with the flow cytometry analysis, compound **28** was more potent than compound **5**, while compound **29** produced no significant change in cleaved PARP at any concentration, suggesting that compound **28** possessed optimal growth inhibitory and pro-apoptotic activities in the SGC7901 cells.

Please insert Figure 5

2.5 In Vivo Antitumor Activity

In consideration of the results from the apoptosis and immunoblotting assays, compound **28** was selected for further evaluation of *in vivo* antitumor efficacy in an SGC-7901 human gastric carcinoma cell xenograft mouse model (**Figure 6**). Nude mice bearing established SGC-7901 tumour xenografts were dosed orally with compound **28** (50 mg/kg or 100 mg/kg daily over a 23-day period). Curcumin (50 mg/kg) was used as a positive control drug. Relative to the vehicle-treated control group, the 100 mg/kg/day dose of compound **28** showed significant *in vivo* antitumor efficacy (48%) and produced no clinical signs of intolerance. Moreover, tumour weight was dose-dependently decreased by compound **28** (**Figure 6B**). During the experiment, no significant loss of body weight was observed in mice treated with compound **28** in comparison with the vehicle control group (**Figure 6C**). Immunohistochemical analysis performed on tumour sections confirmed that treatment with compound **28** significantly decreased cell proliferation (Ki67 staining) and increased apoptosis (cleaved-caspase-3) in the tumour-bearing mice (**Figure 7**).

Please insert Figure 6

Please insert Figure 7

3. Conclusion

In this study, we reported the synthesis of a series of long-chain alkoxyated MCACs and evaluation of their biological activity. All of the compounds showed inhibitory effects towards gastrointestinal carcinoma cells, which were superior to that of curcumin. Compounds **5**, **28**, and **29** showed strong inhibition of SGC-7901 cells, which was superior to that produced by curcumin. The anti-proliferative activity of the test compounds in gastrointestinal carcinoma cells was tested using the MTS assay. As expected, the IC₅₀s of the test compounds were much lower than that of curcumin. In addition, compounds **5**, **28**, and **29** induced apoptosis in SGC-7901 cells more potently than curcumin. Furthermore, compounds **5**, **28**, and **29** exhibited the ability to upregulate cleaved PARP and downregulate expression of caspase-3 and Bcl-2 in SGC-7901 cells, while curcumin did not produce the same effects. Moreover, compound **28** exhibited significant tumour inhibition in an SGC-7901-driven xenograft mouse model. These results indicate that compound **28** has advantages over other compounds, as demonstrated by its

anti-proliferative effect against gastrointestinal carcinoma cells lines and its significant induction of apoptosis and regulation of apoptosis-related genes in SGC-7901 cells. The preliminary biological activity screening tests of our novel series of curcumin derivatives also indicated that long-chain alkoxyated MACs might serve as potential agents for the treatment of gastric cancer.

4. Material and Methods

4.1. Chemical synthesis

4.1.1. Materials and methods

Solvents were distilled and dried by standard methods. All chemicals were obtained from sigma-aldrich and were used without further purification. All reactions were monitored by thin-layer chromatography (250 silica gel 60 F₂₅₄ glass plates). ¹H NMR and ¹³C NMR spectra were recorded on Bruker 600 MHz instruments, and the chemical shifts were presented in terms of parts per million with TMS as the internal reference. Electron-spray ionization mass spectra in positive mode (ESI-MS) data were obtained with a Bruker Esquire 3000⁺ spectrometer. Chromatographic purification was carried out on Silica Gel 60 (E. Merck, 70-230 mesh).

4.1.2. General procedure for synthesis of X2

To a solution of *p*-hydroxybenzaldehyde or vanillin (1mmol) and anhydrous K₂CO₃ (3mmol.) in 20 ml DMF was added requisite linear chain aliphatic dibromoalkanes (5mmol.). The reaction mixture was then stirred at 80°C for 1h, cooled to 0 °C on an ice bath, quenched with 1N HCl and then extracted with CHCl₃. The organic layer was washed with water and dried over Na₂SO₄. Excess solvent was evaporated under reduced pressure and the resultant solid left was purified by column chromatography over silica gel using EtOAc/Hexane as the eluent to afford corresponding substituted aldehydes X2. (Yield: 67.5% and 75.3%)

4.1.3. General procedure for synthesis of X3

K₂CO₃ (7.58mmol) and desired amines (4.54mmol) were added to a stirred solution of substituted benzaldehydes X2 (3.79mmol) in MeCN (15mL). The reaction mixture was then stirred at 80°C for 6h and progress of reaction was monitored by TLC. After completion, it was cooled on ice bath and then extracted with CHCl₃. The organic layer was washed with water and dried over Na₂SO₄. Excess solvent was evaporated under reduced pressure to obtain oily residue of corresponding amino substituted aldehydes X3, which were used for further reaction. (Yield: 26.3%-69.7%)

4.1.4. General procedure for synthesis of I-22

Cyclopentanone or Cyclohexanone (7.5mmol) was added to MeOH (5ml) with amino substituted

benzaldehydes X3 (15mmol) inside. The solution was stirred for 15 min at room temperature followed by dropwise addition of 20% (w/v) aq. NaOH solution. The reaction mixture was stirred at room temperature and monitored by TLC. After completion of reaction, saturated solution of NH₄Cl was added to the reaction mixture. The formed precipitate was washed with water, cold methanol and finally with cold acetone. It was then dried and recrystallized with ethanol/water system to obtain corresponding curcumin derivatives **1-22**. (Yield: 15.4%-72.9%)

4.1.4.1 (2E,6E)-2,6-bis[3-methoxy-4-(3-morpholinopropoxy)benzylidene]cyclohexanone (1)

Yellow powder, m.p: 107.9–109.5 °C. ¹H-NMR (600 MHz, CDCl₃): δ (ppm) 7.726 (2H, s, -CH=×2), 7.067 (2H, d, *J* = 8.4 Hz, Ar-H⁶×2), 7.007 (2H, s, Ar-H²×2), 6.909 (2H, d, *J* = 8.4 Hz, Ar-H⁵×2), 4.121 (4H, t, *J* = 6.6 Hz, Ar-OCH₂-×2), 3.872 (6H, s, -OCH₃×2), 3.754 (8H, t, *J* = 4.2 Hz, morpholine-H^{3,5}×2), 2.927 (4H, t, *J* = 6 Hz, cyclohexanone-H^{3,5}), 2.624 (4H, t, *J* = 7.2 Hz, Ar-OCCCH₂-×2), 2.582 (8H, t, *J* = 4.2 Hz, morpholine-H^{2,6}×2), 2.070-2.093 (4H, m, Ar-OCCH₂-×2), 1.810-1.823 (2H, m, cyclohexanone-H⁴). ESI-MS *m/z*: 621.6 (M+1)⁺, calcd for C₃₆H₄₈N₂O₇: 620.8.

4.1.4.2 (2E,6E)-2-[4-(3-bromopropoxy)-3-methoxybenzylidene]-6-[3-methoxy-4-(3-morpholinopropoxy)benzylidene]cyclohexanone (2)

Yellow oil. ¹H-NMR (600 MHz, CDCl₃): δ (ppm) 7.734 (2H, s, -CH=×2), 7.021 (2H, d, *J* = 9.6 Hz, Ar_A-H⁶, Ar_B-H⁶), 6.960 (2H, s, Ar_A-H², Ar_B-H²), 6.916 (2H, d, *J* = 9.6 Hz, Ar_A-H⁵, Ar_B-H⁵), 4.118 (4H, t, *J* = 7.2 Hz, Ar_A-OCH₂-, Ar_B-OCH₂-), 3.879 (6H, s, -OCH₃×2), 3.744 (6H, m, morpholine-H^{3,5}, Br-CH₂-), 2.923 (4H, t, *J* = 6.6 Hz, cyclohexanone-H^{3,5}), 2.596 (2H, t, *J* = 7.2 Hz, Ar-OCCCH₂-), 2.532 (4H, t, *J* = 4.8 Hz, morpholine-H^{2,6}), 2.356-2.389 (2H, m, Br-CCH₂C-), 2.063-2.083 (2H, m, Ar-OCCH₂-), 1.910-1.928 (2H, m, cyclohexanone-H⁴). ESI-MS *m/z*: 615.4 (M+1)⁺, calcd for C₃₂H₄₀BrNO₆: 614.6.

4.1.4.3 (2E,6E)-2,6-bis{4-[3-(dipropylamino)propoxy]-3-methoxybenzylidene}cyclohexanone(3)

Yellow oil. ¹H-NMR (600 MHz, CDCl₃): δ (ppm) 7.723 (2H, s, -CH=×2), 7.076 (2H, d, *J* = 8.4 Hz, Ar-H⁶×2), 7.000 (2H, s, Ar-H²×2), 6.897 (2H, d, *J* = 8.4 Hz, Ar-H⁵×2), 4.119 (4H, t, *J* = 5.4 Hz, -OCH₂C-×2), 3.865 (6H, s, -OCH₃×2), 2.915 (4H, t, *J* = 6.6 Hz, cyclohexanone-H^{3,5}), 2.651-2.717 (12H, m, NCH₂-×6), 2.152 (4H, m, -OCCH₂C-×2), 1.611-1.649 (10H, m, -NCCH₂-×4, cyclohexanone-H⁴), 0.939 (12H, t, *J* = 7.2 Hz, -CH₃×4). ESI-MS *m/z*: 649.7 (M+1)⁺, calcd for C₄₀H₆₀N₂O₅:648.9.

4.1.4.4 (2E,6E)-2,6-bis[3-methoxy-4-[3-(4-methylpiperazin-1-yl)propoxy]benzylidene]cyclohexanone(4)

Yellow powder, m.p: 94.5-96.1 °C. ¹H-NMR (600 MHz, DMSO-d₆): δ (ppm) 7.567 (2H, s, -CH=×2), 7.138 (2H, s, Ar-H²×2), 7.058 (2H, d, *J* = 8.4 Hz, Ar-H⁶×2), 6.958 (2H, d, *J* = 8.4 Hz, Ar-H⁵×2), 4.009 (4H, t, *J* = 7.2 Hz,

-OCH₂C-×2), 3.782 (6H, s, -OCH₃×2), 2.905 (4H, t, *J* = 6 Hz, cyclohexanone-H^{3,5}), 2.624 (4H, t, *J* = 7.2 Hz, -OCCCH₂-×2), 2.483 (16H, s, piperazine-H^{2,3,5,6}×2), 2.154 (6H, s, NCH₃×2), 1.812-1.877 (4H, m, -OCCH₂CN-×2), 1.148-1.162 (2H, m, cyclohexanone-H⁴). ESI-MS *m/z*: 647.7 (M+1)⁺, calcd for C₃₈H₅₄N₄O₅:646.8.

4.1.4.5 (2E,6E)-2,6-bis[4-[3-(diethylamino)propoxy]-3-methoxybenzylidene]cyclohexanone(5)

Yellow powder, m.p: 294.2-295.6 °C. ¹H-NMR (600 MHz, DMSO-d₆): δ (ppm) 7.579 (2H, s, -CH=×2), 7.122 (2H, s, Ar-H²×2), 7.103 (2H, d, *J* = 8.4 Hz, Ar-H⁶×2), 7.003 (2H, d, *J* = 8.4 Hz, Ar-H⁵×2), 4.021 (4H, t, *J* = 6 Hz, -OCH₂C-×2), 3.790 (6H, s, -OCH₃×2), 2.890 (4H, t, *J* = 5.4 Hz, cyclohexanone-H^{3,5}), 2.419-2.454 (12H, m, -NCH₂-×6), 1.792-1.814 (6H, m, -OCCH₂C-×2, cyclohexanone-H⁴), 0.926 (12H, t, *J* = 6.6 Hz, -NCCH₃×4). ¹³C-NMR (600 MHz, DMSO-d₆): δ (ppm) 188.512, 149.012×2, 148.685×2, 135.860×2, 134.237×2, 128.103×2, 123.823×2, 114.412×2, 112.629×2, 66.548×2, 55.629×2, 48.626×2, 46.418×4, 27.901×2, 26.613×2, 22.509, 11.768×4. ESI-MS *m/z*: 593.7 (M+1)⁺, calcd for C₃₆H₅₂N₂O₅: 592.8.

4.1.4.6 (2E,6E)-2,6-bis[4-[3-(1H-imidazol-1-yl)propoxy]-3-methoxybenzylidene]cyclohexanone(6)

Yellow oil. ¹H-NMR (600 MHz, DMSO-d₆): δ (ppm) 7.617 (2H, s, imidazole-H²×2), 7.588 (2H, s, Ar-CH=×2), 7.158-7.195 (4H, m, Ar-H^{2,6}×2), 7.106 (2H, d, *J* = 7.8 Hz, imidazole-H⁵×2), 7.009 (2H, d, *J* = 8.4 Hz, Ar-H⁵×2), 6.891 (2H, d, *J* = 7.8 Hz, imidazole-H⁴×2), 4.136 (8H, t, *J* = 6.6 Hz, -OCH₂CCH₂-×2), 3.810 (6H, s, -OCH₃×2), 2.901 (4H, t, *J* = 5.4 Hz, cyclohexanone-H^{3,5}), 2.169-2.191 (4H, m, -OCCH₂C-), 1.179-1.701 (2H, m, cyclohexanone-H⁴). ESI-MS *m/z*: 583.7 (M+1)⁺, calcd for C₃₄H₃₈N₄O₅:582.7.

4.1.4.7 (2E,6E)-2,6-bis[3-methoxy-4-[3-(piperidin-1-yl)propoxy]benzylidene]cyclohexanone(7)

Yellow powder, m.p: 192.3-193.4 °C. ¹H-NMR (600 MHz, DMSO-d₆): δ (ppm) 7.583(2H, s, -CH=×2), 7.132 (2H, s, Ar-H²×2), 7.113 (2H, d, *J* = 8.4 Hz, Ar-H⁶×2), 7.025 (2H, d, *J* = 8.4 Hz, Ar-H⁵×2), 4.031 (4H, t, *J* = 6.6 Hz, OCH₂×2), 3.798(6H, s, -OCH₃×2), 2.909 (4H, t, *J* = 6 Hz, cyclohexanone-H^{3,5}), 2.384-2.413 (12H, m, NCH₂×6), 2.128-2.144 (4H, m, OCCH₂C-×2), 1.848-1.865 (14H, m, piperidine-H^{3,4,5}×2, cyclohexanone-H⁴). ESI-MS *m/z*: 617.9 (M+1)⁺, calcd for C₃₈H₅₂N₂O₅:616.8.

4.1.4.8 (2E,6E)-2,6-bis[4-(3-bromopropoxy)-3-methoxybenzylidene]cyclohexanone(8)

Yellow powder, m.p: 123.7-124.4 °C. ¹H-NMR (600 MHz, DMSO-d₆): δ (ppm) 7.589 (2H, s, -CH=×2), 7.151 (2H, s, Ar-H²×2), 7.130 (2H, d, *J* = 9 Hz, Ar-H⁶×2), 7.025 (2H, d, *J* = 9 Hz, Ar-H⁵×2), 4.118 (4H, t, *J* = 6 Hz, OCH₂×2), 3.810 (6H, s, -OCH₃×2), 3.661 (4H, t, *J* = 6.6 Hz, BrCH₂-×2), 2.909 (4H, t, *J* = 4.8 Hz, cyclohexanone-H^{3,5}), 2.255-2.267 (4H, m, BrCCH₂-×2), 1.690-1.710 (2H, m, cyclohexanone-H⁴). ESI-MS *m/z*: 608.9 (M+1)⁺, calcd for

C₂₈H₃₂Br₂O₅: 608.3.

4.1.4.9 (2E,6E)-2-[4-(3-bromopropoxy)-3-methoxybenzylidene]-6-[4-[3-(diethylamino)propoxy]-3-methoxybenzylidene]cyclohexanone(9)

Yellow oil. ¹H-NMR (600 MHz, DMSO-d₆): δ (ppm) 7.542 (2H, s, Ar_A-CH=C-, Ar_B-CH=C-), 7.196 (2H, s, Ar_A-H², Ar_B-H²), 7.142 (2H, d, *J* = 8.4 Hz, Ar_A-H⁶, Ar_B-H⁶), 6.975 (2H, d, *J* = 8.4 Hz, Ar_A-H⁵, Ar_B-H⁵), 4.022 (4H, m, Ar_A-OCH₂C-, Ar_B-OCH₂C-), 3.911 (6H, s, -OCH₃×2), 3.675 (2H, t, *J* = 6 Hz, BrCH₂-), 3.108-3.125 (4H, m, -NCH₂C×2), 2.930 (4H, t, *J* = 6.6 Hz, cyclohexanone-H^{3,5}), 2.398 (2H, t, *J* = 6 Hz, Ar_B-OCCCH₂-), 2.162-2.184 (2H, m, BrCCH₂-), 2.013-2.025 (2H, m, Ar_B-OCCH₂C-), 1.720-1.734 (2H, m, cyclohexanone-H⁴), 1.189 (6H, s, -NCCH₃×2). ESI-MS *m/z*: 601.4 (M+1)⁺, calcd for C₃₂H₄₂BrNO₅:600.6.

4.1.4.10 (2E,6E)-2-[4-(3-bromopropoxy)-3-methoxybenzylidene]-6-[3-methoxy-4-[3-(piperidin-1-yl)propoxy]benzylidene]cyclohexanone(10)

Yellow oil. ¹H-NMR (600 MHz, DMSO-d₆): δ (ppm) 7.571 (2H, s, Ar_A-CH=C-, Ar_B-CH=C-), 7.142-7.160 (4H, m, Ar_A-H^{2,6}, Ar_B-H^{2,6}), 7.028 (2H, d, *J* = 8.4 Hz, Ar_A-H⁵, Ar_B-H⁵), 4.085 (2H, t, *J* = 6 Hz, Ar_A-OCH₂C-), 3.992 (2H, t, *J* = 6.6 Hz, Ar_B-OCH₂C-), 3.811 (6H, s, -OCH₃×2), 3.789 (2H, t, *J* = 6 Hz, BrCH₂-), 2.884 (4H, t, *J* = 6 Hz, cyclohexanone-H^{3,5}), 2.301-2.367 (6H, m, NCH₂×2), 1.870-1.893 (2H, m, -OCCH₂CBr), 1.823-1.859 (2H, m, Ar_B-OCCH₂C-), 1.447-1.484 (8H, m, piperidine-H^{3,4,5}, cyclohexanone-H⁴). ESI-MS *m/z*: 613.4 (M+1)⁺, calcd for C₃₃H₄₂BrNO₅: 612.6.

4.1.4.11 (2E,6E)-2-[4-(3-bromopropoxy)-3-methoxybenzylidene]-6-[3-methoxy-4-[3-(4-methylpiperazin-1-yl)propoxy]benzylidene]cyclohexanone (11)

Yellow oil. ¹H-NMR (600 MHz, DMSO-d₆): δ (ppm) 7.576 (2H, s, Ar_A-CH=C-, Ar_B-CH=C-), 7.512 (2H, d, *J* = 8.4 Hz, Ar_A-H⁶, Ar_B-H⁶), 7.388 (2H, s, Ar_A-H², Ar_B-H²), 7.168 (2H, d, *J* = 8.4 Hz, Ar_A-H⁵, Ar_B-H⁵), 4.103 (2H, t, *J* = 6.6 Hz, Ar_A-OCH₂C-), 4.027 (2H, t, *J* = 7.2 Hz, Ar_B-OCH₂C-), 3.828(6H, s, -OCH₃×2), 3.754 (2H, t, *J* = 6.6 Hz, BrCH₂), 2.539 (4H, t, *J* = 6 Hz, cyclohexanone-H^{3,5}), 2.402 (2H, t, *J* = 6.6 Hz, piperazine-CH₂-), 2.140 (8H, s, piperazine-H^{2,3,5,6}), 1.972-1.986 (5H, m, -OCCH₂CBr-, NCH₃), 1.878-1.901 (2H, m, Ar_B-OCCH₂C-), 1.161-1.185 (2H, m, cyclohexanone-H⁴). ESI-MS *m/z*: 628.5 (M+1)⁺, calcd for C₃₃H₄₃BrN₂O₅: 627.6.

4.1.4.12 (2E,6E)-2,6-bis[4-(2-bromoethoxy)-3-methoxybenzylidene]cyclohexanone(12)

Yellow powder, m.p: 199.8-200.9 °C. ¹H-NMR (600 MHz, DMSO-d₆): δ(ppm) 7.592 (2H, s, -CH=×2), 7.167 (2H, s, Ar-H²×2), 7.122 (2H, d, *J* = 8.4 Hz, Ar-H⁶×2), 7.054 (2H, d, *J* = 8.4 Hz, Ar-H⁵×2), 4.355 (4H, t, *J* = 5.4 Hz, -OCH₂×2), 3.822 (6H, s, -OCH₃×2), 3.789(4H, t, *J* = 6 Hz, -CH₂Br×2), 2.910 (4H, t, *J* = 6 Hz,

cyclohexanone-H^{3,5}), 1.722-1.740 (2H, m, cyclohexanone-H⁴). ESI-MS m/z : 581.0 (M+1)⁺, calcd for C₂₆H₂₈Br₂O₅: 580.0.

4.1.4.13 (2E,6E)-2,6-bis[4-(2-bromoethoxy)benzylidene]cyclohexanone(13)

Yellow powder, m.p: 101.3-102.7°C. ¹H-NMR (600 MHz, DMSO-d₆): δ (ppm) 7.582 (2H, s, -CH=×2), 7.519 (4H, d, $J = 8.4$ Hz, Ar-H^{2,6}×2), 7.044 (4H, d, $J = 8.4$ Hz, Ar-H^{3,5}×2), 4.380 (4H, t, $J = 5.4$ Hz, -OCH₂CBr-×2), 3.822(4H, t, $J = 5.4$ Hz, -OCCH₂Br-×2), 2.876 (4H, t, $J = 4.8$ Hz, cyclohexanone-H^{3,5}), 1.128-1.171 (2H, m, cyclohexanone-H⁴). ESI-MS m/z : 521.3 (M+1)⁺, calcd for C₂₄H₂₄Br₂O₃: 520.3.

4.1.4.14 (2E,5E)-2-{4-[3-(1H-imidazol-1-yl)propoxy]-3-methoxybenzylidene}-5-[4-(3-bromopropoxy)-3-methoxybenzylidene]cyclopentanone(14)

Yellow oil. ¹H-NMR (600 MHz, DMSO-d₆): δ(ppm) 7.699 (1H, s, imidazole-H²), 7.399 (2H, s, Ar-CH=C-×2), 7.295-7.229 (5H, m, Ar-H^{2,6}×2, imidazole-H⁵), 7.059 (2H, d, $J = 8.4$ Hz, Ar-H⁵×2), 6.936 (1H, d, $J = 7.8$ Hz, imidazole-H⁴), 4.140-4.163 (6H, m, -OCH₂CCBr-, -OCH₂CCH₂N-), 3.869 (6H, s, -OCH₃×2), 3.671 (2H, t, $J = 6$ Hz, -OCCCH₂Br), 3.094 (4H, s, cyclopentanone-H^{4,5}), 2.197-2.216 (4H, m, -OCCH₂CBr, -OCCH₂CN-). ESI-MS m/z : 582.3 (M+1)⁺, calcd for C₃₀H₃₃BrN₂O₅: 581.5.

4.1.4.15 (2E,5E)-2,5-bis[4-(3-bromopropoxy)-3-methoxybenzylidene]cyclopentanone(15)

Yellow powder, m.p: 137.6-139.1°C. ¹H-NMR (600 MHz, CDCl₃): δ (ppm) 7.542 (2H, s, -CH=×2), 7.227 (2H, d, $J = 8.4$ Hz, Ar-H⁶×2), 7.139 (2H, s, Ar-H²×2), 6.975 (2H, d, $J = 8.4$ Hz, Ar-H⁵×2), 4.220 (4H, t, $J = 6$ Hz, -OCH₂-×2), 3.910 (6H, s, -OCH₃×2), 3.639 (4H, t, $J = 6$ Hz, -CH₂Br×2), 3.115 (4H, s, cyclopentanone-H^{3,4}), 2.377-2.417 (4H, m, -OCCH₂CBr×2). ESI-MS m/z : 595.1 (M+1)⁺, calcd for C₂₇H₃₀Br₂O₅: 594.3.

4.1.4.16 (2E,5E)-2,5-bis[4-[3-(1H-imidazol-1-yl)propoxy]-3-methoxybenzylidene]cyclopentanone(16)

Yellow powder, m.p: 127.3-129.2°C. ¹H-NMR (600 MHz, CDCl₃): δ (ppm) 7.538 (2H, s, imidazole-H²×2), 7.512 (2H, s, Ar-CH=×2), 7.187 (2H, d, $J = 7.8$ Hz, Ar-H⁶×2), 7.147 (2H, s, Ar-H²×2), 7.060 (2H, d, $J = 8.4$ Hz, imidazole-H⁵×2), 6.937 (2H, d, $J = 7.8$ Hz, Ar-H⁵×2), 6.875 (2H, d, $J = 8.4$ Hz, imidazole-H⁴×2), 4.230 (4H, t, $J = 6$ Hz, -OCH₂-×2), 3.990 (4H, t, $J = 6$ Hz, -OCCCH₂-×2), 3.934 (6H, s, -OCH₃×2), 3.111 (4H, s, cyclopentanone-H^{3,4}), 2.313-2.271 (4H, m, -OCCH₂-×2). ESI-MS m/z : 648.92 (M-1)⁻. ESI-MS m/z : 569.8 (M+1)⁺, calcd for C₃₃H₃₆N₄O₅: 568.7.

4.1.4.17 (2E,5E)-2,5-bis[3-methoxy-4-(3-morpholinopropoxy)benzylidene]cyclopentanone(17)

Yellow powder, m.p: 176.4-177.8°C ¹H-NMR (600 MHz, DMSO-d₆): δ(ppm) 7.375 (2H, s, -CH=×2), 7.253 (2H,

d, $J = 7.2$ Hz, Ar-H⁶×2), 7.215 (2H, s, Ar-H²×2), 7.059 (2H, d, $J = 7.2$ Hz, Ar-H⁵×2), 4.049 (4H, t, $J = 6.6$ Hz, -OCH₂-×2), 3.809 (6H, s, -OCH₃×2), 3.554 (8H, t, $J = 4.2$ Hz, morpholine-H^{3,5}×2), 3.079 (4H, s, cyclopentanone-H^{3,4}), 2.522 (4H, t, $J = 6.6$ Hz, Ar-OCCCH₂-×2), 2.483 (8H, t, $J = 4.2$ Hz, morpholine-H^{2,6}×2), 1.132-1.148 (4H, m, -OCCH₂C-×2). ESI-MS m/z : 607.7 (M+1)⁺, calcd for C₃₅H₄₆N₂O₇: 606.8.

4.1.4.18 (2E,5E)-2,5-bis[3-methoxy-4-[3-(piperidin-1-yl)propoxy]benzylidene]cyclopentanone(18)

Yellow powder, m.p: 198.3-200.2 °C. ¹H-NMR (600 MHz, DMSO-d₆): δ(ppm) 7.402 (2H, s, -CH=×2), 7.287 (2H, s, Ar-H²×2), 7.270 (2H, d, $J = 8.4$ Hz, Ar_A-H⁶×2), 7.085 (2H, d, $J = 8.4$ Hz, Ar-H⁵×2), 4.079 (4H, t, $J = 6$ Hz, -OCH₂-), 3.835 (6H, s, -OCH₃×2), 3.100 (4H, s, cyclopentanone-H^{3,4}), 2.560-2.702 (12H, m, NCH₂-×6), 1.976-1.995 (4H, m, -OCCH₂C-×2), 1.442-1.586 (12H, m, piperidine-H^{3,4,5}×2). ESI-MS m/z : 603.7 (M+1)⁺, calcd for C₃₇H₅₀N₂O₅: 602.8.

4.1.4.19 (2E,5E)-2-[4-(3-bromopropoxy)-3-methoxybenzylidene]-5-[3-methoxy-4-[3-(piperidin-1-yl)propoxy]benzylidene]cyclopentanone(19)

Yellow oil. ¹H-NMR (600 MHz, DMSO-d₆): δ(ppm) 7.410 (2H, s, Ar_A-CH=, Ar_B-CH=), 7.340-7.385 (4H, m, Ar_A-H^{2,6}, Ar_B-H^{2,6}), 6.980 (2H, d, $J = 8.4$ Hz, Ar_A-H⁵, Ar_B-H⁵), 4.162 (2H, t, $J = 5.4$ Hz, Ar_A-OCH₂C-), 4.089 (2H, t, $J = 6$ Hz, Ar_B-OCH₂C-), 3.870 (6H, s, -OCH₃×2), 3.573 (2H, t, $J = 5.4$ Hz, -CH₂Br), 3.110 (4H, s, cyclopentanone-H^{3,4}), 2.370-2.412 (6H, m, NCH₂-×3), 2.245-2.307 (2H, m, -OCCH₂CBr), 1.967-1.980 (2H, m, piperidine-CCH₂-), 1.321-1.413 (6H, m, piperidine-H^{3,4,5}). ESI-MS m/z : 599.3 (M+1)⁺, calcd for C₃₂H₄₀BrNO₅: 598.6.

4.1.4.20 (2E,5E)-2,5-bis[4-(2-bromoethoxy)-3-methoxybenzylidene]cyclopentanone(20)

Yellow powder, m.p: 155.2-156.9°C. ¹H-NMR (600 MHz, DMSO-d₆): δ(ppm) 7.406 (2H, s, -CH=×2), 7.307 (2H, s, Ar-H²×2), 7.265 (2H, d, $J = 8.4$ Hz, Ar_A-H⁶×2), 7.097 (2H, d, $J = 8.4$ Hz, Ar-H⁵×2), 4.376 (4H, t, $J = 5.4$ Hz, -OCH₂-×2), 3.851 (6H, s, -OCH₃×2), 3.820 (4H, t, $J = 5.4$ Hz, -CH₂Br×2), 3.100 (4H, s, cyclopentanone-H^{3,4}). ESI-MS m/z : 567.5 (M+1)⁺, calcd for C₂₅H₂₆Br₂O₅: 566.3.

4.1.4.21 (2E,5E)-2,5-bis[4-(2-bromoethoxy)benzylidene]cyclopentanone(21)

Yellow powder, m.p: 206.3-207.6°C. ¹H-NMR (600 MHz, DMSO-d₆): δ(ppm) 7.662 (4H, d, $J = 9$ Hz, Ar-H^{2,6}×2), 7.401 (2H, s, -CH=×2), 7.086 (4H, d, $J = 9$ Hz, Ar-H^{3,5}×2), 4.402 (4H, t, $J = 5.4$ Hz, -OCH₂CBr×2), 3.833 (4H, t, $J = 5.4$ Hz, -OCCH₂Br×2), 3.063 (4H, s, cyclopentanone-H^{3,4}). ESI-MS m/z : 507.1 (M+1)⁺, calcd for C₂₃H₂₂Br₂O₃: 506.2.

4.1.4.22 (1E,4E)-1,5-bis[3-methoxy-4-(3-morpholinopropoxy)phenyl]penta-1,4-dien-3-one(22)

Yellow oil. ¹H-NMR (600 MHz, DMSO-d₆): δ(ppm) 7.688 (2H, d, *J* = 15.6 Hz, Ar-CH=C-×2), 7.136-7.153 (4H, m, Ar-H^{2,6}×2), 7.022-7.043 (4H, m, Ar-C=CH-×2, Ar-H⁵×2), 4.058 (4H, t, *J* = 6 Hz, -OCH₂-×2), 3.842 (6H, s, -OCH₃×2), 3.564 (8H, t, *J* = 5.4 Hz, morpholine-H^{3,5}×2), 2.409 (4H, t, *J* = 6 Hz, -OCCCH₂-×2), 2.360 (8H, t, *J* = 5.4 Hz, morpholine-H^{2,6}×2), 1.831-1.904 (4H, m, -OCCH₂C×2). ESI-MS *m/z*: 581.8 (M+1)⁺, calcd for C₃₃H₄₄N₂O₇: 580.7.

4.1.5. General procedure for synthesis of X4

Amino substituted benzaldehydes X3 were dissolved in acetone and followed by dropwise addition of 20% (w/v) aq. NaOH solution. The mixture was stirred at room temperature for 3h. Excess acetone was evaporated under reduced pressure and the residue was extracted with ethyl acetate and the organic layer washed with brine, dried over anhydrous magnesium sulphate, and concentrated under vacuum. The solid was purified by chromatography over silica gel using ethyl acetate/petroleum ether as the eluent to give compounds X4.

4.1.6. General procedure for synthesis of 23-37

A reaction mixture of the compound X4 (1.0 equiv), substituted benzaldehydes (1.0 equiv) and 20% (w/v) aq. NaOH (0.1 equiv) in MeOH was stirred at room temperature and monitored by TLC. After completion of reaction, saturated solution of NH₄Cl was added to the reaction mixture. The formed precipitate was washed with water, cold methanol and finally with cold acetone. It was then dried and recrystallized with ethanol/water system to obtain corresponding curcumin derivatives **23-37**. (Yield:24.3%-76.8%)

4.1.6.1 (1E,4E)-1-(2-chlorophenyl)-5-[3-methoxy-4-(3-morpholinopropoxy)phenyl]penta-1,4-dien-3-one(23)

Yellow powder, m.p: 135.6-137.4°C. ¹H-NMR (600 MHz, CDCl₃): δ (ppm) 8.110 (1H, d, *J* = 15.6 Hz, Ar_B-CH=C-), 7.714 (1H, d, *J* = 15.6 Hz, Ar_A-CH=C-), 7.528 (1H, d, *J* = 7.2 Hz, Ar_B-H³), 7.384 (1H, d, *J* = 7.2 Hz, Ar_B-H⁶), 7.302-7.329 (2H, m, Ar_A-H² Ar_B-H⁵), 7.133-7.211 (3H, m, Ar_A-H^{5,6}, Ar_B-H⁴), 7.054 (1H, d, *J* = 15.6 Hz, Ar_A-C=CH-), 6.969 (1H, d, *J* = 15.6 Hz, Ar_B-C=CH-), 4.162 (2H, t, *J* = 7.2 Hz, -OCH₂-), 3.913 (3H, s, -OCH₃), 3.810 (4H, s, morpholine-H^{3,5}), 2.230 (2H, t, *J* = 7.2 Hz, -OCCCH₂-), 2.309 (4H, s, morpholine-H^{2,6}), 1.405-1.444 (2H, m, -OCCH₂C-). ESI-MS *m/z*: 441.95 (M-1)⁻. ESI-MS *m/z*: 443.0 (M+1)⁺, calcd for C₂₅H₂₈ClNO₄: 442.0.

4.1.6.2 (1E,4E)-1-(2-fluoro-4-methoxyphenyl)-5-[3-methoxy-4-(3-morpholinopropoxy)phenyl]penta-1,4-dien-3-one(24)

Red oil. ¹H-NMR (600 MHz, CDCl₃): δ(ppm) 7.719 (1H, d, *J* = 16.2 Hz, Ar_B-CH=C-), 7.670 (1H, d, *J* = 16.2 Hz, Ar_A-CH=C-), 7.542 (1H, d, *J* = 8.4 Hz, Ar_B-H⁶), 7.178 (1H, d, *J* = 8.4Hz, Ar_A-H⁶), 7.135 (1H, s, Ar_A-H²),

7.075 (1H, d, $J = 16.2$ Hz, $\text{Ar}_A\text{-C}=\text{CH-}$), 6.900-6.947 (3H, m, $\text{Ar}_B\text{-H}^3$, $\text{Ar}_A\text{-H}^5$, $\text{Ar}_B\text{-C}=\text{CH-}$), 6.743 (1H, d, $J = 8.4$ Hz, $\text{Ar}_B\text{-H}^5$), 4.155 (2H, t, $J = 6.6$ Hz, $-\text{OCH}_2-$), 3.915 (3H, s, $\text{Ar}_A\text{-OCH}_3$), 3.845 (3H, s, $\text{Ar}_B\text{-OCH}_3$), 3.806 (4H, s, morpholine- $\text{H}^{3,5}$), 2.505 (2H, t, $J = 6.6$ Hz, $-\text{OCCCH}_2-$), 2.214 (4H, s, morpholine- $\text{H}^{2,4}$), 1.251-1.313 (2H, m, $-\text{OCCH}_2\text{C-}$). ESI-MS m/z : 456.6 ($\text{M}+1$)⁺, calcd for $\text{C}_{26}\text{H}_{30}\text{FNO}_5$: 455.5.

4.1.6.3 (1E,4E)-1-(3,4-dimethoxyphenyl)-5-[3-methoxy-4-(3-morpholinopropoxy)phenyl]penta-1,4-dien-3-one (25)

Yellow oil. ¹H-NMR (600 MHz, CDCl_3): δ (ppm) 7.707 (1H, d, $J = 15.6$ Hz, $\text{Ar}_B\text{-CH}=\text{C-}$), 7.531 (1H, d, $J = 15.6$ Hz, $\text{Ar}_A\text{-CH}=\text{C-}$), 7.198-7.173 (4H, m, $\text{Ar}_B\text{-H}^2$, $\text{Ar}_B\text{-H}^6$, $\text{Ar}_A\text{-H}^2$, $\text{Ar}_A\text{-H}^6$), 6.987-6.870 (4H, m, $\text{Ar}_B\text{-H}^5$, $\text{Ar}_A\text{-H}^5$, $\text{Ar}_A\text{-C}=\text{CH-}$, $\text{Ar}_B\text{-C}=\text{CH-}$), 4.295 (2H, t, $J = 7.2$ Hz, $-\text{OCH}_2-$), 4.081 (6H, s, $\text{Ar}_A\text{-OCH}_3$, $\text{Ar}_B\text{-3-OCH}_3$), 4.070 (3H, s, $\text{Ar}_B\text{-4-OCH}_3$), 3.921 (4H, s, morpholine- $\text{H}^{3,5}$), 2.520 (2H, t, $J = 7.2$ Hz, $-\text{OCCCH}_2-$), 2.293 (4H, s, morpholine- $\text{H}^{2,6}$), 1.386-1.437 (2H, m, $-\text{OCCH}_2-$). ESI-MS m/z : 467.5 ($\text{M}+1$)⁺, calcd for $\text{C}_{27}\text{H}_{33}\text{NO}_6$: 467.6.

4.1.6.4 (1E,4E)-1-[3-methoxy-4-(3-morpholinopropoxy)phenyl]-5-(2,4,6-trimethoxyphenyl)penta-1,4-dien-3-one (26)

Yellow powder, m.p: 125.4-126.7°C. ¹H-NMR (600 MHz, DMSO-d_6): δ (ppm) 7.995 (1H, d, $J = 15.6$ Hz, $\text{Ar}_B\text{-CH}=\text{C-}$), 7.534 (1H, d, $J = 15.6$ Hz, $\text{Ar}_A\text{-CH}=\text{C-}$), 7.393 (1H, s, $\text{Ar}_A\text{-H}^2$), 6.947-7.205 (3H, m, $\text{Ar}_A\text{-H}^5$, $\text{Ar}_A\text{-H}^6$, $\text{Ar}_A\text{-C}=\text{CH-}$), 6.655 (1H, s, $J = 15.6$ Hz, $\text{Ar}_B\text{-C}=\text{CH-}$), 6.213 (2H, s, $\text{Ar}_B\text{-H}^3$, $\text{Ar}_B\text{-H}^5$), 4.038 (2H, t, $J = 7.2$ Hz, $-\text{OCH}_2-$), 3.906 (6H, s, $\text{Ar}_B\text{-2,6-OCH}_3$), 3.854 (3H, s, $\text{Ar}_A\text{-OCH}_3$), 3.833 (3H, s, $\text{Ar}_B\text{-4-OCH}_3$), 3.560 (4H, s, morpholine- $\text{H}^{3,5}$), 2.393 (2H, t, $J = 7.2$ Hz, $-\text{OCCCH}_2-$), 2.350 (4H, s, morpholine- $\text{H}^{2,6}$), 1.860-1.884 (2H, m, $-\text{OCCH}_2-$). ESI-MS m/z : 498.3 ($\text{M}+1$)⁺, calcd for $\text{C}_{28}\text{H}_{35}\text{NO}_7$: 497.6.

4.1.6.5 (1E,4E)-1-mesityl-5-[3-methoxy-4-(3-morpholinopropoxy)phenyl]penta-1,4-dien-3-one (27)

White powder, m.p: 137.5-139.1°C. ¹H-NMR (600 MHz, CDCl_3): δ (ppm) 7.878 (1H, d, $J = 16.2$ Hz, $\text{Ar}_B\text{-CH}=\text{C-}$), 7.649 (1H, d, $J = 16.2$ Hz, $\text{Ar}_A\text{-CH}=\text{C-}$), 7.123 (1H, s, $\text{Ar}_A\text{-H}^2$), 6.884-6.917 (5H, m, $\text{Ar}_A\text{-H}^{5,6}$, $\text{Ar}_B\text{-H}^{3,5}$, $\text{Ar}_A\text{-C}=\text{CH-}$), 6.713 (1H, d, $J = 16.2$ Hz, $\text{Ar}_B\text{-C}=\text{CH-}$), 4.153 (2H, t, $J = 6$ Hz, $-\text{OCH}_2-$), 3.909 (3H, s, $-\text{OCH}_3$), 3.838 (4H, s, morpholine- $\text{H}^{3,5}$), 2.376 (6H, s, $\text{Ar}_B\text{-2-CH}_3$, $\text{Ar}_B\text{-6-CH}_3$), 2.298 (3H, s, $\text{Ar}_B\text{-4-CH}_3$), 2.260 (2H, t, $J = 6$ Hz, $-\text{OCCCH}_2-$), 2.206 (4H, s, morpholine- $\text{H}^{2,6}$), 2.035-2.054 (2H, m, $-\text{OCCH}_2\text{C-}$). ESI-MS m/z : 450.5($\text{M}+1$)⁺, calcd for $\text{C}_{28}\text{H}_{35}\text{NO}_4$: 449.6.

4.1.6.6 (1E,4E)-1-[3-methoxy-4-(3-morpholinopropoxy)phenyl]-5-(2-methoxyphenyl)penta-1,4-dien-3-one (28)

Yellow powder, m.p: 113.2-124.1°C. ¹H-NMR (600 MHz, CDCl_3): δ (ppm) 8.040 (1H, d, $J = 15.6$ Hz, $\text{Ar}_B\text{-CH}=\text{C-}$), 7.652 (1H, d, $J = 15.6$ Hz, $\text{Ar}_A\text{-CH}=\text{C-}$), 7.585 (1H, d, $J = 7.8$ Hz, $\text{Ar}_B\text{-H}^6$), 7.323-7.349 (1H, m,

Ar_B-H⁴), 7.112-7.163 (3H, m, Ar_A-H², Ar_A-H⁶, Ar_B-H³), 6.882-6.965 (4H, m, Ar_A-H⁵, Ar_B-H⁵, Ar_A-C=CH-, Ar_B-C=CH-), 4.110 (2H, t, *J* = 6 Hz, -OCH₂C-), 3.890 (3H, s, Ar_A-OCH₃), 3.862 (3H, s, Ar_B-OCH₃), 3.703 (4H, s, morpholine-H^{3,5}), 2.530 (2H, t, *J* = 6 Hz, -OCCCH₂-), 2.461 (4H, s, morpholine-H^{2,6}), 2.012-2.054 (2H, m, -OCCH₂C-). ¹³C-NMR (600 MHz, CDCl₃): δ (ppm) 188.802, 158.108, 150.270, 149.075×2, 142.492, 137.745, 131.149, 128.266, 127.485, 125.715, 123.265, 122.444, 120.266, 112.184, 110.729, 110.106, 66.694, 66.366×4, 55.539, 53.162×2, 25.632. ESI-MS *m/z*: 438.3(M+1)⁺, calcd for C₂₆H₃₁NO₅: 437.5.

4.1.6.7 (1E,4E)-1-(2,3-dimethoxyphenyl)-5-[3-methoxy-4-(3-morpholinopropoxy)phenyl]penta-1,4-dien-3-one (29)

Yellow oil. ¹H-NMR (600 MHz, DMSO-d₆): δ(ppm) 8.016(1H, d, *J* = 16.2 Hz, Ar_B-CH=C-), 7.798(1H, d, *J* = 16.2 Hz, Ar_A-CH=C-), 7.383 (1H, d, *J* = 7.8 Hz, Ar_B-H⁶), 7.224 (1H, s, Ar_A-H²), 7.099-7.112 (1H, m, Ar_B-H⁵), 7.040-7.099 (4H, m, Ar_A-H^{5,6}, Ar_A-C=CH-, Ar_B-C=CH-), 6.925 (1H, t, *J* = 7.8 Hz, Ar_B-H⁴), 4.098 (2H, t, *J* = 6.6 Hz, -OCH₂C-), 3.838 (6H, s, Ar_A-3-OCH₃, Ar_B-3-OCH₃), 3.796 (3H, s, Ar_B-2-OCH₃), 3.561 (4H, s, morpholine-H^{3,5}), 2.407 (2H, t, *J* = 6.6 Hz, -OCCCH₂-), 2.380 (4H, s, morpholine-H^{2,6}), 1.901-1.940 (2H, m, -OCCH₂C-). ¹³C-NMR (600 MHz, DMSO-d₆): δ (ppm) 188.712, 153.022, 152.700, 148.797×2, 147.487, 147.133, 141.769, 126.878, 124.230×2, 121.015, 120.553, 120.380, 119.136, 114.179, 112.134, 69.710, 66.451×2, 65.577×2, 62.299, 61.313, 56.035, 55.884, 27.243. ESI-MS *m/z*: 468.7 (M+1)⁺, calcd for C₂₇H₃₃NO₆: 467.6.

4.1.6.8 (1E,4E)-1-[4-(3-bromopropoxy)-3-methoxyphenyl]-5-(2-methoxyphenyl)penta-1,4-dien-3-one(30)

Yellow oil. ¹H-NMR (600 MHz, DMSO-d₆): δ(ppm) 7.958 (1H, d, *J* = 15.6 Hz, Ar_B-CH=C-), 7.81 (1H, d, *J* = 7.2 Hz, Ar_B-H⁶), 7.746 (1H, d, *J* = 15.6 Hz, Ar_A-CH=C-), 7.305-7.436 (2H, m, Ar_A-H², Ar_B-H⁴), 7.009-7.175 (6H, m, Ar_A-H^{5,6}, Ar_B-H^{3,5}, Ar_A-C=CH-, Ar_B-C=CH-), 4.123 (2H, t, *J* = 6 Hz, -OCH₂-), 3.886 (3H, s, Ar_B-OCH₃), 3.849 (3H, s, Ar_A-OCH₃), 3.658 (2H, t, *J* = 6 Hz, BrCH₂-), 1.972-1.990 (2H, m, BrCCH₂C-). ESI-MS *m/z*: 431.9(M+1)⁺, calcd for C₂₂H₂₃BrO₄: 431.3.

4.1.6.9 (1E,4E)-1-[4-(2-bromoethoxy)-3-methoxyphenyl]-5-(2-methoxyphenyl)penta-1,4-dien-3-one(31)

Yellow powder, m.p: 116.6-117.9°C. ¹H-NMR (600 MHz, CDCl₃): δ(ppm) 8.068 (1H, d, *J* = 16.2 Hz, Ar_B-CH=C-), 7.671 (1H, d, *J* = 15.6 Hz, Ar_A-CH=C-), 7.619 (1H, d, *J* = 7.2 Hz, Ar_B-H⁶), 7.364-7.390 (1H, m, Ar_B-H⁴), 7.132-7.199 (2H, m, Ar_A-H^{2,6}), 6.909-7.005 (5H, m, Ar_A-H⁵, Ar_B-H^{3,5}, Ar_A-C=CH-, Ar_B-C=CH-), 4.378 (2H, t, *J* = 6.6 Hz, -OCH₂-), 3.935 (3H, s, Ar_B-OCH₃), 3.922 (3H, s, Ar_A-OCH₃), 3.681 (2H, t, *J* = 6.6 Hz, Br-CH₂-). ESI-MS *m/z*: 418.0(M+1)⁺, calcd for C₂₁H₂₁BrO₄: 417.3.

4.1.6.10 (1E,4E)-1-[4-(tert-butyl)phenyl]-5-[3-methoxy-4-(3-morpholinopropoxy)phenyl]penta-1,4-dien-3-one

(32)

Yellow oil. $^1\text{H-NMR}$ (600 MHz, DMSO- d_6): δ (ppm) 7.705 (1H, d, $J = 15.6$ Hz, $\text{Ar}_B\text{-CH=C-}$), 7.665 (1H, d, $J = 15.6$ Hz, $\text{Ar}_A\text{-CH=C-}$), 7.532 (2H, d, $J = 8.4$ Hz, $\text{Ar}_B\text{-H}^{2,6}$), 7.400 (2H, d, $J = 8.4$ Hz, $\text{Ar}_B\text{-H}^{3,5}$), 7.147 (1H, d, $J = 8.4$ Hz, $\text{Ar}_A\text{-H}^6$), 7.122 (1H, s, $\text{Ar}_A\text{-H}^2$), 7.047 (1H, d, $J = 15.6$ Hz, $\text{Ar}_B\text{-C=CH-}$), 6.936 (1H, d, $J = 15.6$ Hz, $\text{Ar}_A\text{-C=CH-}$), 6.881 (1H, d, $J = 8.4$ Hz, $\text{Ar}_A\text{-H}^5$), 4.106 (2H, t, $J = 6.6$ Hz, $-\text{OCH}_2\text{C-}$), 3.888 (3H, s, $-\text{OCH}_3$), 3.715 (4H, s, morpholine- $\text{H}^{3,5}$), 2.560 (2H, t, $J = 7.2$ Hz, $-\text{OCCCH}_2\text{-}$), 2.495 (4H, s, morpholine- $\text{H}^{2,6}$), 2.023-2.069 (2H, m, $-\text{OCCH}_2\text{C-}$), 1.310 (9H, s, $-\text{CCH}_3 \times 3$). ESI-MS m/z : 464.7 ($\text{M}+1$) $^+$, calcd for $\text{C}_{29}\text{H}_{37}\text{NO}_4$: 463.6.

4.1.6.11 (1E,4E)-1-[3-methoxy-4-(3-morpholinopropoxy)phenyl]-5-[2-(trifluoromethyl)phenyl]penta-1,4-dien-3-one(33)

Yellow oil. $^1\text{H-NMR}$ (600 MHz, DMSO- d_6): δ (ppm) 8.125 (1H, d, $J = 15.6$ Hz, $\text{Ar}_B\text{-CH=C-}$), 7.808 (1H, d, $J = 15.6$ Hz, $\text{Ar}_A\text{-CH=C-}$), 7.387-7.719 (4H, m, $\text{Ar}_A\text{-H}^2$, $\text{Ar}_B\text{-H}^{3,5,6}$), 6.832-7.135 (4H, m, $\text{Ar}_A\text{-H}^{5,6}$, $\text{Ar}_B\text{-H}^4$, $\text{Ar}_A\text{-C=CH-}$), 6.683 (1H, d, $J = 15.6$ Hz, $\text{Ar}_B\text{-C=CH-}$), 4.218 (2H, d, $J = 6.6$ Hz, $-\text{OCH}_2\text{C-}$), 3.827 (3H, s, $-\text{OCH}_3$), 3.792 (4H, s, morpholine- $\text{H}^{3,5}$), 2.360 (2H, t, $J = 6.6$ Hz, $-\text{OCCCH}_2\text{-}$), 2.301 (4H, s, morpholine- $\text{H}^{2,6}$), 1.821-1.909 (2H, m, $-\text{OCCH}_2\text{C-}$). ESI-MS m/z : 476.4 ($\text{M}+1$) $^+$, calcd for $\text{C}_{26}\text{H}_{28}\text{F}_3\text{NO}_4$: 475.5.

4.1.6.12 (2E,6E)-2-(2,3-dimethoxybenzylidene)-6-[3-methoxy-4-(3-morpholinopropoxy)benzylidene]cyclohexanone(34)

Red oil. $^1\text{H-NMR}$ (600 MHz, DMSO- d_6): δ (ppm) 7.712 (1H, s, $\text{Ar}_B\text{-CH=}$), 7.682 (1H, s, $\text{Ar}_A\text{-CH=}$), 7.512-7.571 (2H, m, $\text{Ar}_A\text{-H}^6$, $\text{Ar}_B\text{-H}^6$), 7.394 (1H, s, $\text{Ar}_A\text{-H}^2$), 7.055-7.161 (3H, m, $\text{Ar}_A\text{-H}^5$, $\text{Ar}_B\text{-H}^{4,5}$), 4.106 (2H, t, $J = 6.6$ Hz, $-\text{OCH}_2\text{-}$), 3.826 (9H, s, $-\text{OCH}_3 \times 3$), 3.560 (4H, s, morpholine- $\text{H}^{3,5}$), 2.898 (4H, t, $J = 6.6$ Hz, cyclohexanone- $\text{H}^{3,5}$), 2.410 (2H, t, $J = 6.6$ Hz, $-\text{OCCCH}_2\text{-}$), 2.352 (4H, s, morpholine- $\text{H}^{2,6}$), 1.891-1.914 (2H, m, $-\text{OCCH}_2\text{C-}$), 1.558-1.650 (2H, m, cyclohexanone- H^4). ESI-MS m/z : 508.3 ($\text{M}+1$) $^+$, calcd for $\text{C}_{30}\text{H}_{37}\text{NO}_6$: 507.6.

4.1.6.13 (2E,6E)-2-(3,4-dimethoxybenzylidene)-6-[3-methoxy-4-(3-morpholinopropoxy)benzylidene]cyclohexanone(35)

Yellow oil. $^1\text{H-NMR}$ (600 MHz, CDCl_3): δ (ppm) 7.732 (2H, s, $-\text{CH}=\times 2$), 7.012-7.112 (4H, m, $\text{Ar}_A\text{-H}^2$, $\text{Ar}_A\text{-H}^6$, $\text{Ar}_B\text{-H}^2$, $\text{Ar}_B\text{-H}^6$), 6.915 (1H, d, $J = 7.2$ Hz, $\text{Ar}_B\text{-H}^5$), 6.903 (1H, d, $J = 7.8$ Hz, $\text{Ar}_A\text{-H}^5$), 4.140 (2H, t, $J = 6$ Hz, $-\text{OCH}_2\text{C-}$), 3.915 (3H, s, $\text{Ar}_A\text{-OCH}_3$), 3.904 (3H, s, $\text{Ar}_B\text{-OCH}_3$), 3.875 (3H, s, $\text{Ar}_B\text{-OCH}_3$), 3.839 (4H, s, morpholine- $\text{H}^{3,5}$), 2.931 (4H, t, $J = 5.4$ Hz, cyclohexanone- $\text{H}^{3,5}$), 2.381 (2H, t, $J = 6$ Hz, $-\text{OCCCH}_2\text{-}$), 3.727 (4H, s, morpholine- $\text{H}^{2,6}$), 1.913-1.928 (2H, m, $-\text{OCCH}_2\text{C-}$), 1.808-1.828 (2H, m, cyclohexanone- H^4). ESI-MS m/z : 508.4 ($\text{M}+1$) $^+$, calcd for $\text{C}_{30}\text{H}_{37}\text{NO}_6$: 507.6.

4.1.6.14 (2E,6E)-2-[3-methoxy-4-(3-morpholinopropoxy)benzylidene]-6-(2-methoxybenzylidene)cyclohexanone(36)

Yellow oil. ¹H-NMR (600 MHz, DMSO-d₆): δ(ppm) 7.790 (1H, s, Ar_B-CH=), 7.701 (1H, d, *J* = 7.2 Hz, Ar_B-H⁶), 7.597 (1H, s, Ar_A-CH=), 7.346-7.370 (1H, m, Ar_B-H⁴), 6.983-7.135 (5H, m, Ar_A-H^{2,5,6}, Ar_B-H^{3,5}), 4.034 (2H, t, *J* = 6.6 Hz, -OCH₂-), 3.826 (3H, s, Ar_B-OCH₃), 3.798 (3H, s, Ar_A-OCH₃), 3.561 (4H, s, morpholine-H^{3,5}), 2.887 (4H, t, *J* = 6.6 Hz, cyclohexanone-H^{3,5}), 2.407 (2H, t, *J* = 6.6 Hz, -OCCCH₂-), 2.346 (4H, s, morpholine-H^{2,6}), 1.858-1.889 (2H, m, -OCCCH₂-), 1.651-1.680 (2H, m, cyclohexanone-H⁴). ESI-MS *m/z*: 478.4 (M+1)⁺, calcd for C₂₉H₃₅NO₅: 477.6.

4.1.6.15 (2E,5E)-2-[3-methoxy-4-(3-morpholinopropoxy)benzylidene]-5-[2-(trifluoromethyl)benzylidene]cyclopentanone(37)

Yellow oil. ¹H-NMR (600 MHz, CDCl₃): δ(ppm) 7.808 (1H, s, Ar_B-CH=C-), 7.714 (1H, d, *J* = 7.8 Hz, Ar_B-H³), 7.327-7.669 (5H, m, Ar_B-CH=C-, Ar_A-H^{2,6}, Ar_B-H^{5,6}), 7.043-7.107 (1H, m, Ar_B-H⁴), 6.938 (1H, d, *J* = 8.4 Hz, Ar_A-H⁵), 4.129 (2H, d, *J* = 6.6 Hz, -OCH₂C-), 3.883 (3H, s, -OCH₃), 3.847 (4H, s, morpholine-H^{3,5}), 3.025 (2H, s, cyclopentanone-H³), 2.952 (2H, s, cyclopentanone-H⁴), 2.557 (2H, t, *J* = 6.6 Hz, -OCCCH₂-), 2.486 (4H, s, morpholine-H^{2,6}), 1.965-2.002 (2H, m, -OCCCH₂C-). ESI-MS *m/z*: 502.1 (M+1)⁺, calcd for C₂₈H₃₀F₃NO₄: 501.5.

4.2 Cell Lines and Culture

Two human gastric carcinoma cell lines SGC-7901 and MGC80-3, human colorectal cancer cell line SW-620, mouse colorectal cancer cell line CT-26, and the human gastric mucosa epithelial cell line GES-1 were obtained from the cell bank of the Chinese Academy of Sciences and grown in RPMI-1640 medium (Gibico) supplemented with 10% (v/v) heat-inactivated fetal bovine serum (Gibico) and antibiotics (100 U/mL penicillin and 100 μg/mL streptomycin). Cells were maintained in a humidified cell incubator at 37°C with 5% CO₂.

4.3 Reagents

Antibodies against Bcl-2(sc-492), Pro-caspase 3 (sc-7148), cleaved PARP (sc-56196), GAPDH (sc-25778) and KI67 (sc-15402) were obtained from Santa Cruz Biotechnology (Santa Cruz, CA); Antibody against Cleaved-caspase 3 (Asp175) was purchased from Cell Signaling Technology

4.4 Cell Growth Inhibition Assays (MTS assay)

Cell lines were seeded in 96-well plates in triplicate at a concentration of 4000 cells / well and allowed to attach overnight. Cells were then exposure to various concentrations of test compounds in triplicate for 72 h under 5% CO₂ at 37°C. MTS ((Promega, San Luis Obispo, CA)) was used according to manufacturer instructions.

Briefly, the MTS solution was added and the culture was incubated for an additional 4 h and absorbance was measured by using the spectraMax M2 microplate reader (MolecularDevices, Sunnyvale, CA) at 490 nm. The results were also expressed as IC₅₀ (the compound concentration required for 50% growth inhibition of tumor cells), which was calculated by the software Origin75. The mean \pm SEM IC₅₀ was determined from the results of three independent tests.

4.5 Cell Apoptosis Assay

Apoptosis was determined using an apoptosis detection Kit (BD Biosciences, USA). Briefly, SGC-7901 cells were seeded into 6-well plates and allowed grown to 80% confluency in complete medium, then cells treated with different concentrations of test compounds for 30h to evaluate the effects of test compounds on apoptosis. Cells were collected, washed twice in ice-cold phosphate-buffered saline (PBS), and then resuspended in binding buffer according to the instructions of the apoptosis Kit. The treated cells (as described above) were simultaneously incubated with fluorescein-labeled Annexin V and PI. Annexin V-binding buffer was then added to the mixture before fluorescence was measured on a FACSCalibur (BD Biosciences; Baltimore, MD, USA). Data were analyzed using Flowjo software.

4.6 Western Blot Analysis

SGC-7901 cells were treated with test compounds for 24 hours, then harvested, washed twice with PBS, lysed on ice for 30min in 80 μ L of lysis buffer to extract total protein, and then centrifuged at 12,000 \times rpm for 15 min. The supernatants were collected from the lysates and the protein concentrations were determined. Aliquots of the lysates (60 μ g of protein) were boiled for 10 min and electrophoresed in 10% sodium dodecyl sulfate-polyacrylamide gel. Separated protein bands were transferred into polyvinylidene fluoride (PVDF) membranes and the membranes were blocked in 5% skimmed milk. The primary antibodies against cleaved-PARP, pro-caspase3 and Bcl-2 were diluted according to the manufacturer's instructions and incubated overnight at 4°C. Horseradish peroxidase-linked secondary antibodies (Santa cruze) were then added at a dilution ratio of 1:300, and incubated at room temperature for 1 h. Protein bands were detected using an EZ-ECL Chemiluminescence Detection Kit (Biological Industries).

4.7 Antitumor effect of compound 28 in xenograft model

Female nude mice were obtained from Animal Center of Wenzhou Medical University (Wenzhou, China) and protocols involving use of animals were approved by the Wenzhou Medical University Animal Policy and Welfare Committee. Eight-week-old female mice were injected subcutaneously with 10 million SGC7901 cells. To determine whether compound 28 inhibits tumor formation after engraftment of cells, treatment was initiated when

tumors reached about 40 mm³, and animals were randomized to receive 0.5% CMCNA alone, compound **28** (50 mg/kg/day, orally), compound **28** (100 mg/kg/day, orally) and curcumin (50mg/kg/day, orally) for 23 consecutive days. Mice were observed daily and tumor size was measured every 2 days using calipers. Volume was calculated using the formula: $\pi/6 \times (\text{large diameter}) \times (\text{small diameter})^2$. Tumor samples and organs were collected when mice were sacrificed. Each sample was cut in halves; one half was preserved in 4% paraformaldehyde and one half was flash-frozen in liquid nitrogen and stored at -80°C until further use.

4.8 Immunohistochemistry

5µm sections were deparaffinized with xylene and rehydrated through graded alcohols into water. Then, antigen retrieval was carried out for 10 minutes in sodium citrate buffer. Tissues were placed in 3% H₂O₂ for 10 minutes to increased permeability, followed by incubation in 1% bovine serum albumin in PBS for 10 minutes, washing twice in PBS. Slides were then incubated with the primary antibodies overnight at 4°C, monoclonal rabbit anti-Ki67 (Santa Cruz, sc-15402) at a 1:50 dilution, cleaved-caspase 3 (Cell Signaling Technology, Asp175) at a 1:100 dilution. Following overnight incubation, slides were washed and incubated with horseradish peroxidase-conjugated secondary antibody for 2h at 37°C with 1:100 dilution. The tissue sections were then washed and stained with DAB substrate-chromogen and then counterstained with hematoxylin, dehydrated, cleared, and mounted with coverslips. Electronic images were captured using microscope.

4.9 Statistical Analysis

Data were presented as the mean ± SEM. Differences between groups were analyzed using the Student's t-test for continuous variables. Statistical analysis was performed using Graphpad prism (version 5) and significance was established at $p < 0.05$.

Acknowledgements

Financial support was provided by the Natural Science Funding of Zhejiang Province (LY13H160022), National Natural Science Foundation of China (81302642, 81402783, and 81473242), Zhejiang Key Health Science and Technology Project (WKJ2013-2-021).

References

- [1] M. Garcia, A. Jemal, E. Ward, M. Center, Y. Hao, R. Siegel, M. Thun, Global cancer facts & figures 2007, Atlanta, GA: American cancer society, 1 (2007).
- [2] F. Kamangar, G.M. Dores, W.F. Anderson, Patterns of cancer incidence, mortality, and prevalence across five continents: defining priorities to reduce cancer disparities in different geographic regions of the world, Journal of

- clinical oncology : official journal of the American Society of Clinical Oncology, 24 (2006) 2137-2150.
- [3] Z.J. Zang, I. Cutcutache, S.L. Poon, S.L. Zhang, J.R. McPherson, J. Tao, V. Rajasegaran, H.L. Heng, N. Deng, A. Gan, K.H. Lim, C.K. Ong, D. Huang, S.Y. Chin, I.B. Tan, C.C. Ng, W. Yu, Y. Wu, M. Lee, J. Wu, D. Poh, W.K. Wan, S.Y. Rha, J. So, M. Salto-Tellez, K.G. Yeoh, W.K. Wong, Y.J. Zhu, P.A. Futreal, B. Pang, Y. Ruan, A.M. Hillmer, D. Bertrand, N. Nagarajan, S. Rozen, B.T. Teh, P. Tan, Exome sequencing of gastric adenocarcinoma identifies recurrent somatic mutations in cell adhesion and chromatin remodeling genes, *Nature genetics*, 44 (2012) 570-574.
- [4] S.C. Oh, Update of adjuvant chemotherapy for resected gastric cancer, *Journal of gastric cancer*, 12 (2012) 3-6.
- [5] D.E.S. A, S. Trastulli, V. Grassi, A. Corsi, I. Barillaro, A. Boccolini, D.I.P. MS, D.I.R. G, A. Santoro, R. Ciocchi, C. Boselli, A. Redler, G. Noya, S.H. Kong, Requirement for a standardised definition of advanced gastric cancer, *Oncology letters*, 7 (2014) 164-170.
- [6] M. Gao, H. Yin, Z.W. Fei, Clinical application of microRNA in gastric cancer in Eastern Asian area, *World journal of gastroenterology : WJG*, 19 (2013) 2019-2027.
- [7] D.M. Parkin, F. Bray, J. Ferlay, P. Pisani, *Global cancer statistics, 2002*, CA: a cancer journal for clinicians, 55 (2005) 74-108.
- [8] H. Brenner, D. Rothenbacher, V. Arndt, Epidemiology of stomach cancer, *Methods in molecular biology*, 472 (2009) 467-477.
- [9] A. Rasul, B. Yu, M. Khan, K. Zhang, F. Iqbal, T. Ma, H. Yang, Magnolol, a natural compound, induces apoptosis of SGC-7901 human gastric adenocarcinoma cells via the mitochondrial and PI3K/Akt signaling pathways, *International journal of oncology*, 40 (2012) 1153-1161.
- [10] S.H. Noh, S.R. Park, H.K. Yang, H.C. Chung, I.J. Chung, S.W. Kim, H.H. Kim, J.H. Choi, H.K. Kim, W. Yu, J.I. Lee, D.B. Shin, J. Ji, J.S. Chen, Y. Lim, S. Ha, Y.J. Bang, C.t. investigators, Adjuvant capecitabine plus oxaliplatin for gastric cancer after D2 gastrectomy (CLASSIC): 5-year follow-up of an open-label, randomised phase 3 trial, *The Lancet. Oncology*, 15 (2014) 1389-1396.
- [11] Y.J. Bang, E. Van Cutsem, A. Feyereislova, H.C. Chung, L. Shen, A. Sawaki, F. Lordick, A. Ohtsu, Y. Omuro, T. Satoh, G. Aprile, E. Kulikov, J. Hill, M. Lehle, J. Ruschoff, Y.K. Kang, G.A.T.I. To, Trastuzumab in combination with chemotherapy versus chemotherapy alone for treatment of HER2-positive advanced gastric or gastro-oesophageal junction cancer (ToGA): a phase 3, open-label, randomised controlled trial, *Lancet*, 376 (2010) 687-697.
- [12] C. Gravalos, A. Jimeno, HER2 in gastric cancer: a new prognostic factor and a novel therapeutic target, *Annals of oncology : official journal of the European Society for Medical Oncology / ESMO*, 19 (2008) 1523-1529.
- [13] D. Ransom, K. Wilson, M. Fournier, R.J. Simes, V. Gebbski, D. Yip, N. Tebbutt, C.S. Karapetis, D. Ferry, S. Gordon, T.J. Price, Final results of Australasian Gastrointestinal Trials Group ARCTIC study: an audit of raltitrexid

for patients with cardiac toxicity induced by fluoropyrimidines, *Annals of oncology : official journal of the European Society for Medical Oncology / ESMO*, 25 (2014) 117-121.

[14] L.H. van Huis-Tanja, H. Gelderblom, C.J. Punt, H.J. Guchelaar, MTHFR polymorphisms and capecitabine-induced toxicity in patients with metastatic colorectal cancer, *Pharmacogenetics and genomics*, 23 (2013) 208-218.

[15] N.A. Bowden, Nucleotide excision repair: why is it not used to predict response to platinum-based chemotherapy?, *Cancer letters*, 346 (2014) 163-171.

[16] M. Scotece, J. Conde, V. Abella, V. Lopez, J. Pino, F. Lago, A.B. Smith, 3rd, J.J. Gomez-Reino, O. Gualillo, New drugs from ancient natural foods. Oleocanthal, the natural occurring spicy compound of olive oil: a brief history, *Drug discovery today*, (2014).

[17] G. Zhang, X. Ye, D. Ji, H. Zhang, F. Sun, C. Shang, Y. Zhang, E. Wu, F. Wang, F. Wu, H. Tian, X. Liu, L. Chen, K. Liu, Y. Wang, H. Liu, W. Zhang, Y. Guan, Q. Wang, X. Zhao, X. Wan, Inhibition of lung tumor growth by targeting EGFR/VEGFR-Akt/NF-kappaB pathways with novel theanine derivatives, *Oncotarget*, 5 (2014) 8528-8543.

[18] M. Sajish, P. Schimmel, A human tRNA synthetase is a potent PARP1-activating effector target for resveratrol, *Nature*, (2014).

[19] C. Zeng, P. Zhong, Y. Zhao, K. Kanchana, Y. Zhang, Z.A. Khan, S. Chakrabarti, L. Wu, J. Wang, G. Liang, Curcumin protects hearts from FFA-induced injury by activating Nrf2 and inactivating NF-kappaB both in vitro and in vivo, *Journal of molecular and cellular cardiology*, 79C (2014) 1-12.

[20] R. Wilken, M.S. Veena, M.B. Wang, E.S. Srivatsan, Curcumin: A review of anti-cancer properties and therapeutic activity in head and neck squamous cell carcinoma, *Molecular cancer*, 10 (2011) 12.

[21] J.S. Jurenka, Anti-inflammatory properties of curcumin, a major constituent of *Curcuma longa*: a review of preclinical and clinical research, *Alternative medicine review : a journal of clinical therapeutic*, 14 (2009) 141-153.

[22] G. Liang, L. Shao, Y. Wang, C. Zhao, Y. Chu, J. Xiao, Y. Zhao, X. Li, S. Yang, Exploration and synthesis of curcumin analogues with improved structural stability both in vitro and in vivo as cytotoxic agents, *Bioorganic & medicinal chemistry*, 17 (2009) 2623-2631.

[23] X. Wang, Y. Wei, S. Yuan, G. Liu, Y. Lu, J. Zhang, W. Wang, Potential anticancer activity of tanshinone IIA against human breast cancer, *International journal of cancer. Journal international du cancer*, 116 (2005) 799-807.

[24] R.J. Youle, A. Strasser, The BCL-2 protein family: opposing activities that mediate cell death, *Nature reviews. Molecular cell biology*, 9 (2008) 47-59.

[25] F. Pettersson, A.G. Dalgleish, R.P. Bissonnette, K.W. Colston, Retinoids cause apoptosis in pancreatic cancer cells via activation of RAR-gamma and altered expression of Bcl-2/Bax, *British journal of cancer*, 87 (2002) 555-561.

[26] J. Bargiela-Iparraguirre, L. Prado-Marchal, N. Pajuelo-Lozano, B. Jimenez, R. Perona, I. Sanchez-Perez, Mad2 and BubR1 modulates tumourigenesis and paclitaxel response in MKN45 gastric cancer cells, *Cell cycle*, 13 (2014) 3590-3601.

[27] C. Soldani, M.C. Lazze, M.G. Bottone, G. Tognon, M. Biggiogera, C.E. Pellicciari, A.I. Scovassi, Poly(ADP-ribose) polymerase cleavage during apoptosis: when and where?, *Experimental cell research*, 269 (2001) 193-201.

Figure legends

Table 1. Inhibition of cell proliferation by compounds in four cancer cell lines and GES-1 gastric mucosa epithelial cell line. The IC₅₀ values were determined as described in “Materials and methods”, Data were obtained from three independent experiments.

Figure 1. The anti-cancer structural-activity relationship of mono-carbonyl analogues of curcumin and the chemical structures of anticancer drugs that including a long-chain alkoxy group.

Figure 2. General synthesis and chemical structures of long-chain alkoxyated mono-carbonyl analogues of curcumin (**1-22**).

Figure 3. General synthesis and chemical structures of long-chain alkoxyated mono-carbonyl analogues of curcumin (**23-37**).

Figure 4. Apoptosis induced by compounds **5**, **28**, **29** treatment in SGC7901 gastric cancer. UR (up right): necrotic cells and late apoptotic cells labeled with PI and Annexin V-FITC. LL (lower left): fully viable cells. LR (lower right): early apoptotic cells labeled with Annexin V-FITC but not with PI. Cells were incubated with the indicated doses (2.5, 5 or 10 μ M) of compounds **5**, **28**, **29** for 30h (DMSO as negative control, cur as positive control), and then harvested and analyzed by flow cytometry. Representative data from one experiment are shown, the average of three separate experiments are shown, significant difference from control was indicated as * character (*p < 0.05).

Figure 5. The expression of cleaved-PARP, Caspase3 and total Bcl-2 after exposure to test compounds in SGC7901 cell. (A) SGC7901 were treated for 24 h with compounds **5**, **28**, **29** at indicated doses (2.5, 5 or 10 μ M) and whole cell extracts were prepared. Protein expression was then analyzed by western blot. (B) cleaved-PARP; (C) Caspase3; (D) Bcl-2. Data are representative of three individual experiments. (* represents p < 0.05)

Figure 6. Schedule dependence of in vivo antitumor activity of compound **28** against the SGC7901 xenograft model. (A) Established (~ 40 mm³) SGC7901 tumors were administered compound **28** on a once (QD x 23, orally) dosing schedule. For comparison, vehicle group of 0.5% CMCNA, positive control group of cur (50 mg/kg, PO) were included. % $\Delta T/\Delta C$ was determined. Data plotted as average tumor volume \pm SEM. Compound **28** causes tumor regressions when dosed at 50 mg/kg/ QD and 100 mg/kg QD schedule. (B) Tumors were weighed after sacrificing the mice on the final day of the study. Compound **28** dose-dependently diminished the tumor weight. (C) Body weights were monitored for the duration of the studies. * indicates $P < 0.05$.

Figure 7. Subcutaneous SGC7901 xenografts, treated with a 50 mg/kg or 100 mg/kg dose of compound **28** were examined KI67 and Cleaved-caspase3 status by immunohistochemistry. Top panel, expression of KI67 in tumor tissue. Representative images were taken from scans at 40x magnification. Bottom panel, expression of Cleaved-caspase3 in tumor tissue. Representative images were taken from scans at 20x magnification.

Table 1

Comp.	IC ₅₀ (μM)				
	SGC7901	MGC803	SW620	CT26	GES-1
1	4.96±1.3	2.06±0.95	1.98±0.08	2.69±0.09	3.02±0.03
2	10.99±0.92	10.24±0.19	5.64±0.9	10.52±0.44	10.04±0.15
4	1.88±0.09	1.94±0.4	1.04±0.06	2.01±0.3	3.27±0.05
5	1.7±0.06	1.72±0.11	0.99±0.02	2.06±0.03	3.45±0.08
6	3.38±0.05	2.21±0.09	2.79±0.07	3.59±0.2	2.87±0.03
7	2.32±0.09	2.92±0.42	2.49±0.15	2.42±0.26	6.35±0.59
9	11.89±1.53	15.48±0.41	4.65±2.42	12.82±0.25	14.08±1.05
12	6.26±2.24	7.72±0.75	6.26±0.62	9.85±0.33	3.56±0.28
16	0.89±0.31	2.46±1.28	0.95±0.53	0.36±0.03	7.09±1.71
17	1±0.1	2.28±0.91	1.49±0.32	0.39±0.05	>30
18	0.44±0.03	0.68±0.08	0.39±0.03	0.18±0.04	0.67±0.18
19	5.08±1.31	7.31±0.03	4.47±0.003	3.86±0.38	7.03±0.003
25	5.99±1.28	7.14±0.22	2.8±0.12	3.13±0.09	7.81±0.26
27	7.67±1.25	8.46±1.16	3.38±0.19	7.01±0.36	8.06±0.33
28	1.91±0.06	2.18±0.41	1.22±0.05	2.56±0.05	2.62±0.19
29	1.84±0.04	2.49±0.25	1.02±0.03	2.38±0.53	2.77±0.01
30	2.84±0.11	6.69±1.05	3.53±0.22	6.39±0.64	4.11±0.25
31	4.52±1.45	5.52±1.34	4.43±0.16	4.51±1.12	4.04±0.18
32	2.77±0.06	2.45±0.44	1.62±0.16	3.26±0.62	3.03±0.02
35	2.87±0.14	8.61±0.5	3.81±0.09	2.99±0.62	8.17±0.43
CUR	24.41±4.76	31.39±13.09	12.52±1.31	7.7±1.05	27.89±2.3

Figure 1

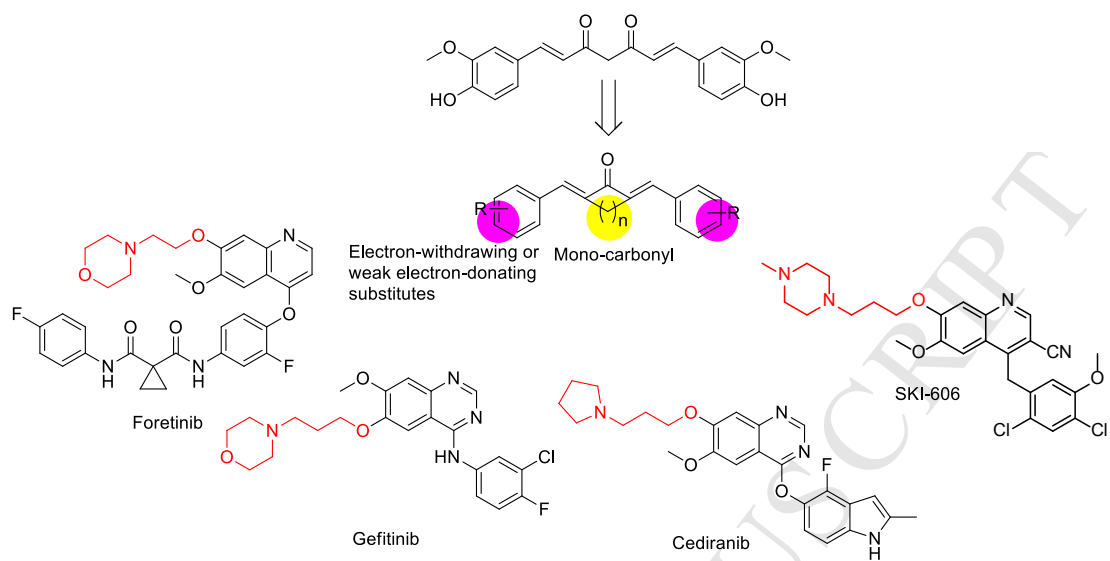


Figure 2

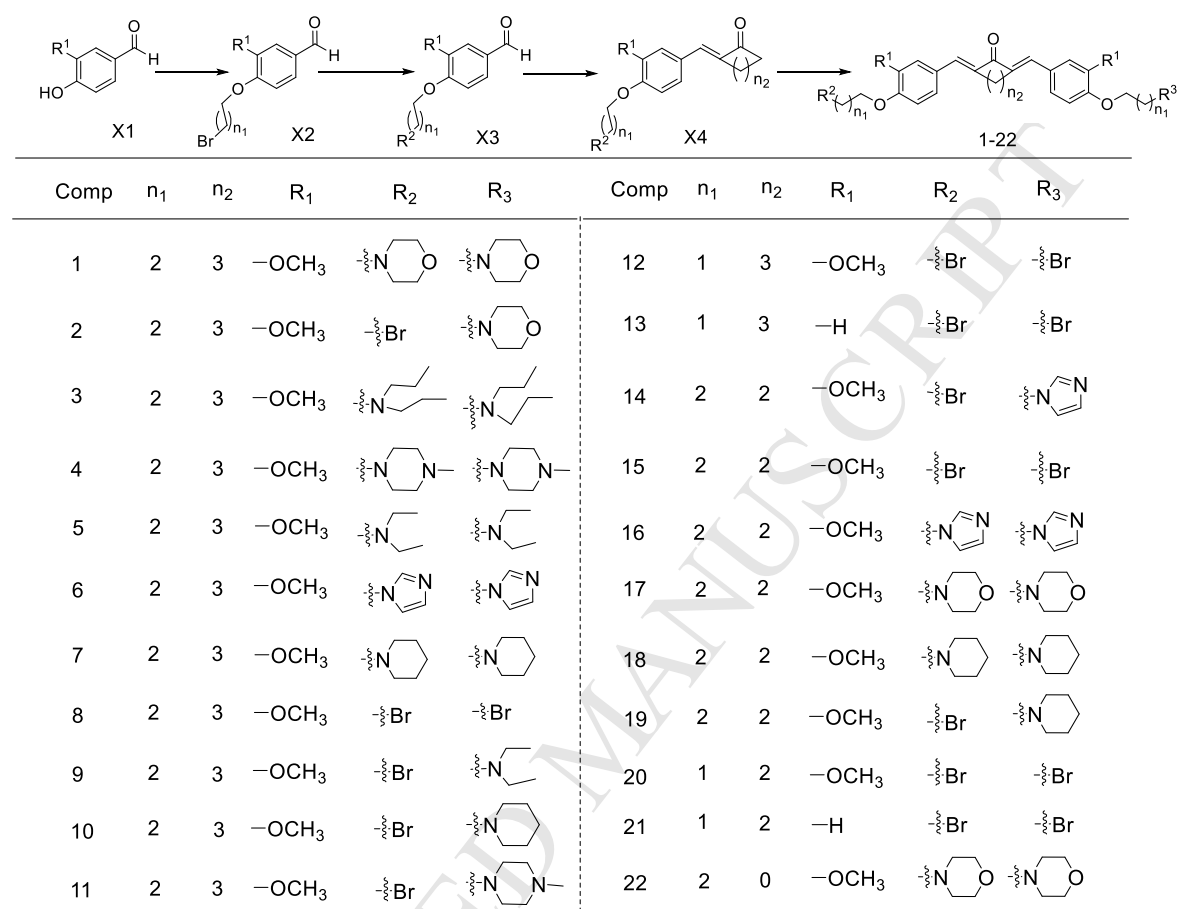
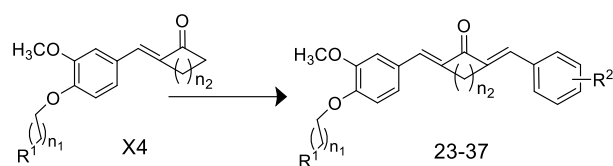


Figure 3



Comp	n ₁	n ₂	R ₁	R ₂	Comp	n ₁	n ₂	R ₁	R ₂
23	2	0		2'-Cl	31	1	0		2'-OCH ₃
24	2	0		2'-F-4'-OCH ₃	32	2	0		4'-C(CH ₃) ₃
25	2	0		3',4'-(OCH ₃) ₂	33	2	0		2'-CF ₃
26	2	0		2',4',6'-(OCH ₃) ₃	34	2	3		2'-CF ₃
27	2	0		2',4',6'-(CH ₃) ₃	35	2	3		3',4'-(OCH ₃) ₂
28	2	0		2'-OCH ₃	36	2	3		3'-OCH ₃
29	2	0		2',3'-(OCH ₃) ₂	37	2	2		2'-CF ₃
30	2	0		2'-OCH ₃					

Figure 4

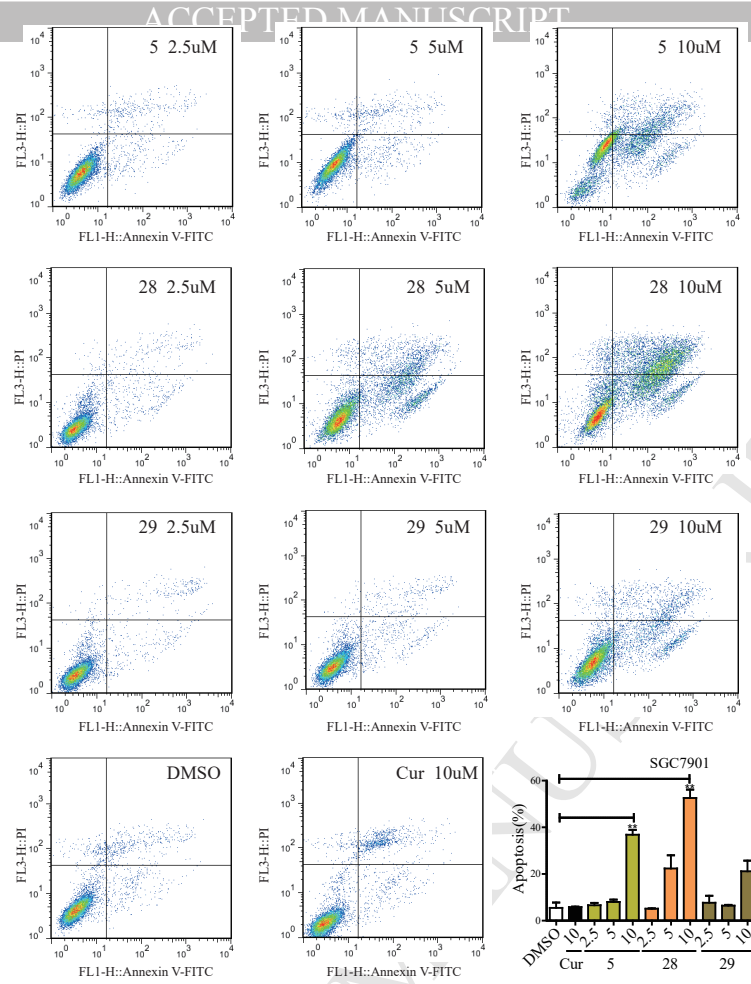


Figure 5

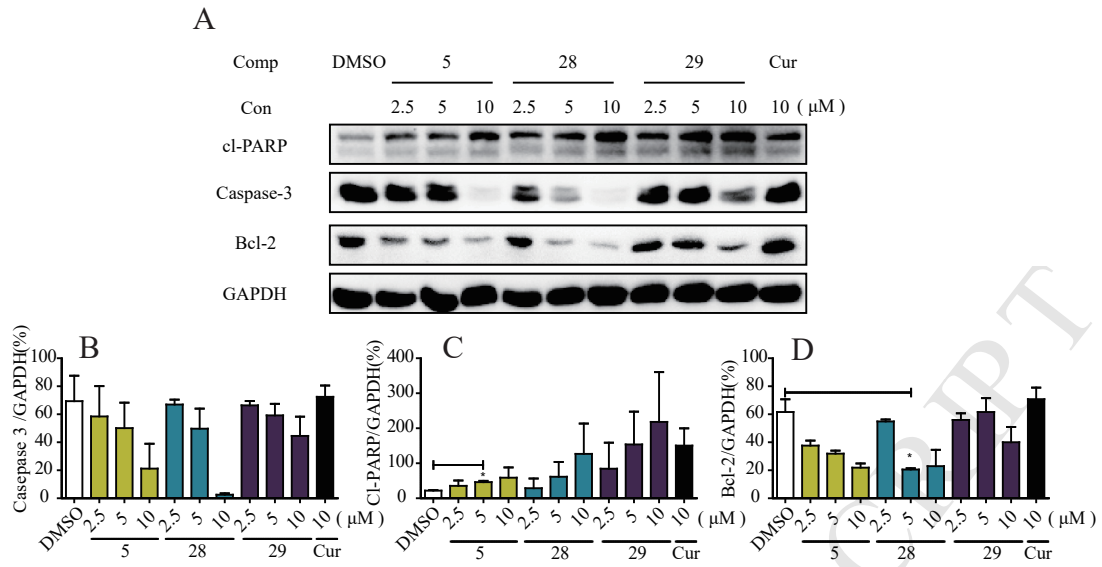


Figure 6

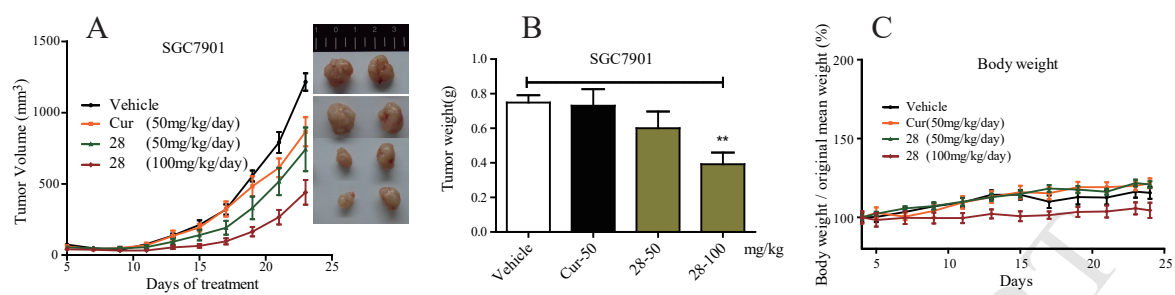
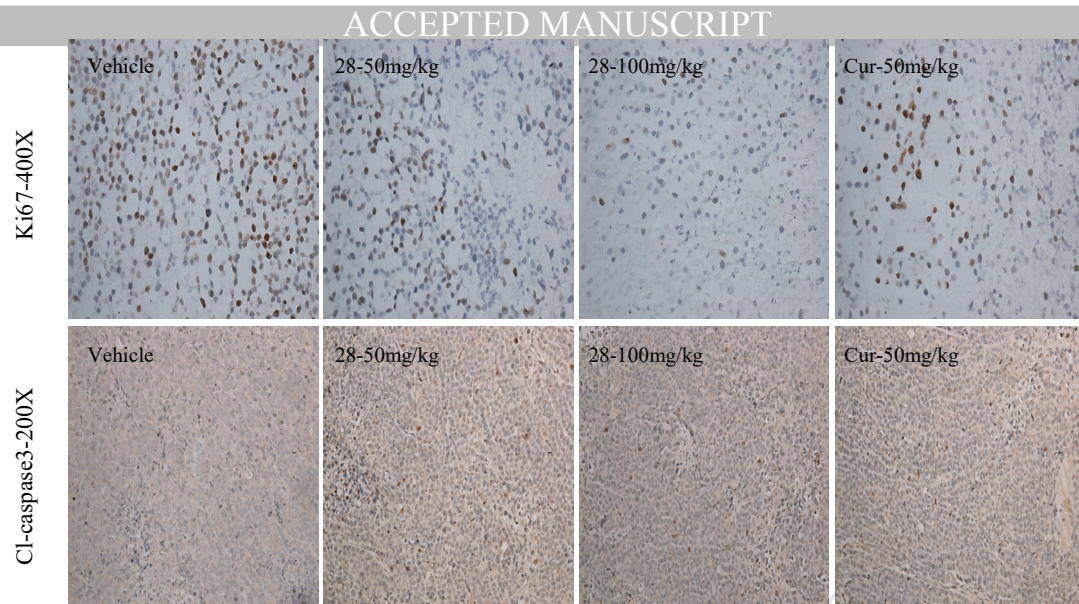


Figure 7



Highlights

1. We synthesized a series of long-chain alkoxyated mono-carbonyl curcumin analogues.
2. The curcumin analogues inhibited tumour cell proliferation and induced apoptosis.
3. The curcumin analogues increased PARP cleavage and down-regulated Bcl-2.
4. Novel curcumin analogue 28 may represent a new treatment for gastric cancer.

Supporting information

Design, Synthesis, and Anticancer Evaluation of Long-chain Alkoxyated Mono-carbonyl Analogues of Curcumin

Qiaoyou Weng^{1,2#}, Lili Fu^{1#}, Gaozhi Chen¹, Junguo Hui², Jingjing Song², Jianpeng Feng¹, Dengjian Shi¹, Yuepiao Cai¹, Jiansong Ji^{2*}, Guang Liang^{1*}

1. Chemical Biology Research Center, School of Pharmaceutical Sciences, Wenzhou Medical University, Wenzhou, Zhejiang 325035, China
2. Department of Interventional Radiology, The Fifth Affiliated Hospital of Wenzhou Medical University, Lishui, Zhejiang 323000, China

#These Authors contributed equally to this work

* Corresponding authors:

Guang Liang, Ph.D, Professor

Director, Chemical Biology Research Center

School of Pharmaceutical Sciences, Wenzhou Medical University

Tel: (+86)-577-86699396; Fax: (+86)-577-86699396

E-mail: wzmcliangguang@163.com

and

Jiansong Ji, Professor

Department of Interventional Radiology, the Fifth Affiliated Hospital of Wenzhou Medical University

E-mail: jjstcty@sina.com

Table S1. Anti-viability activity screen of 37 compounds against four gastric cancer cell lines.

Comp.	Con	Inhibition (%)			
		MGC803	SGC7901	CT26	SW620
1	10 μ M	78.11	81.83	93.28	85.66
2	10 μ M	51.17	61.9	65.23	72.72
3	10 μ M	-18.43	2.83	8.04	10.33
4	10 μ M	77.45	84.8	109.38	86.72
5	10 μ M	80.36	77.99	91.94	82.6
6	10 μ M	88.48	85.04	90.9	82.42
7	10 μ M	76.86	82.83	93.2	86.88
8	10 μ M	-8.68	18.94	49.81	61.17
9	10 μ M	87.03	86.44	92.32	85.32
10	10 μ M	26.86	24.44	61.2	50.01
11	10 μ M	-7.15	15.67	37.33	48.09
12	10 μ M	58.43	69.25	77.3	66.32
13	10 μ M	0.05	10.78	58.34	0.12
14	10 μ M	7.1	14.03	87.12	65.67
15	10 μ M	5.56	6.48	71.02	27.42
16	10 μ M	16.26	76.78	100.93	93.52
17	10 μ M	83.88	86.12	92.53	86.03
18	10 μ M	86.64	84.24	91.93	83.84
19	10 μ M	91.36	88.97	90.25	84.52
20	10 μ M	8.38	20.4	58.63	38.52
21	10 μ M	52.02	75.98	88.07	78.45
22	10 μ M	44.55	67.47	89.68	83.99
23	10 μ M	38.49	75.29	87.2	81.63
24	10 μ M	3.64	51.61	67.57	79.27
25	10 μ M	53.77	66.08	79.65	84.75
26	10 μ M	5.96	9.22	65.83	33.89
27	10 μ M	80.65	78.14	89.56	83.59
28	10 μ M	80.28	75.26	103.73	105.13
29	10 μ M	77.64	73.72	88.9	82.14
30	10 μ M	80.14	74.82	77.24	81.45
31	10 μ M	76.23	78.71	70.48	83.73
32	10 μ M	84.16	76.24	90.65	84.77
33	10 μ M	-2.85	3.22	-24.04	-3.21
34	10 μ M	-9.26	-6.53	57.18	22.47
35	10 μ M	89.78	86.38	86.47	83.6
36	10 μ M	2.3	-0.33	31.65	22.88
37	10 μ M	4.98	29.74	4.71	34.88

Solubility assay of compounds using an UV-visible spectrometer

Compound **5**, **16**, **18**, **28** and **29** were dissolved in a mixed solution containing an equal volume of methanol and water and the maximum absorption wavelength were tested by scan in 200 ~ 600 nm. A series concentrations of those compounds were prepared in a mixed solution with an equal volume of methanol and water and their absorption at maximum absorption wavelength were tested to afford a standard curve. Saturated solutions which obtained from the filtered supersaturated aqueous solution through 0.22 μ m microporous-membrane were diluted with an equal volume of methanol and tested the absorption at the maximum absorption wavelength. Base on the absorption, the concentration of the compounds are determined on the standard curve, and then calculate the concentration of the compound in water to get the solubility.

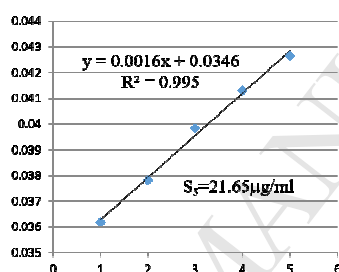


Figure S1 standard curve and solubility of compound 5

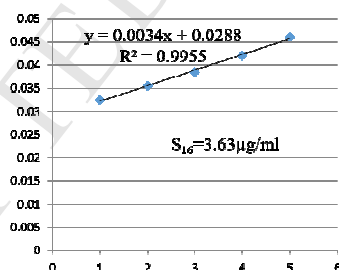


Figure S2 standard curve and solubility of compound 16

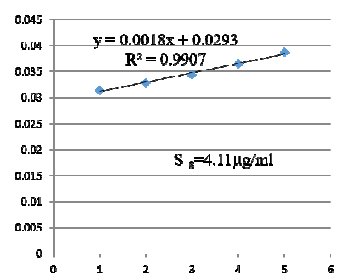


Figure S3 standard curve and solubility of compound 18

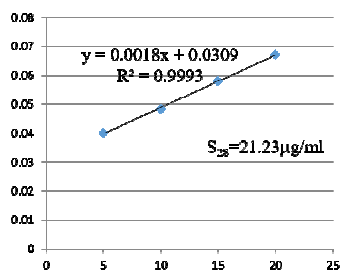


Figure S4 standard curve and solubility of compound 28

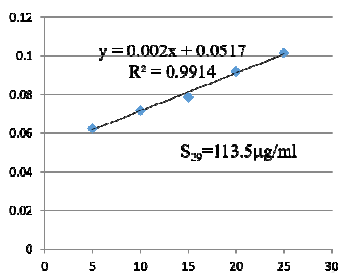
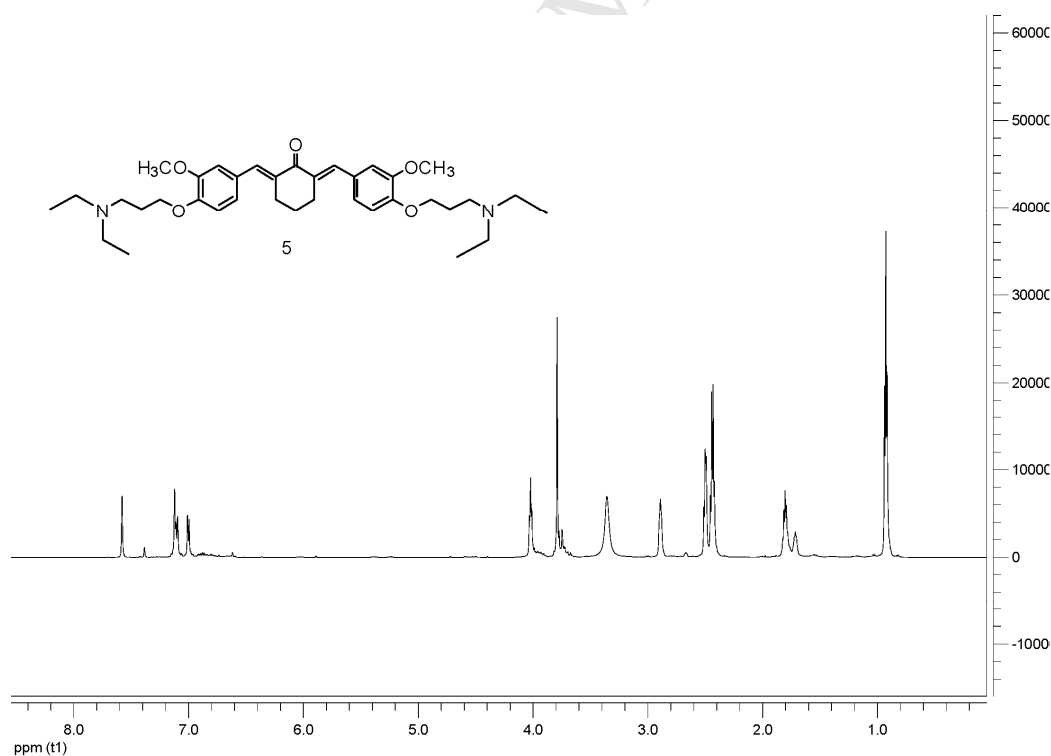
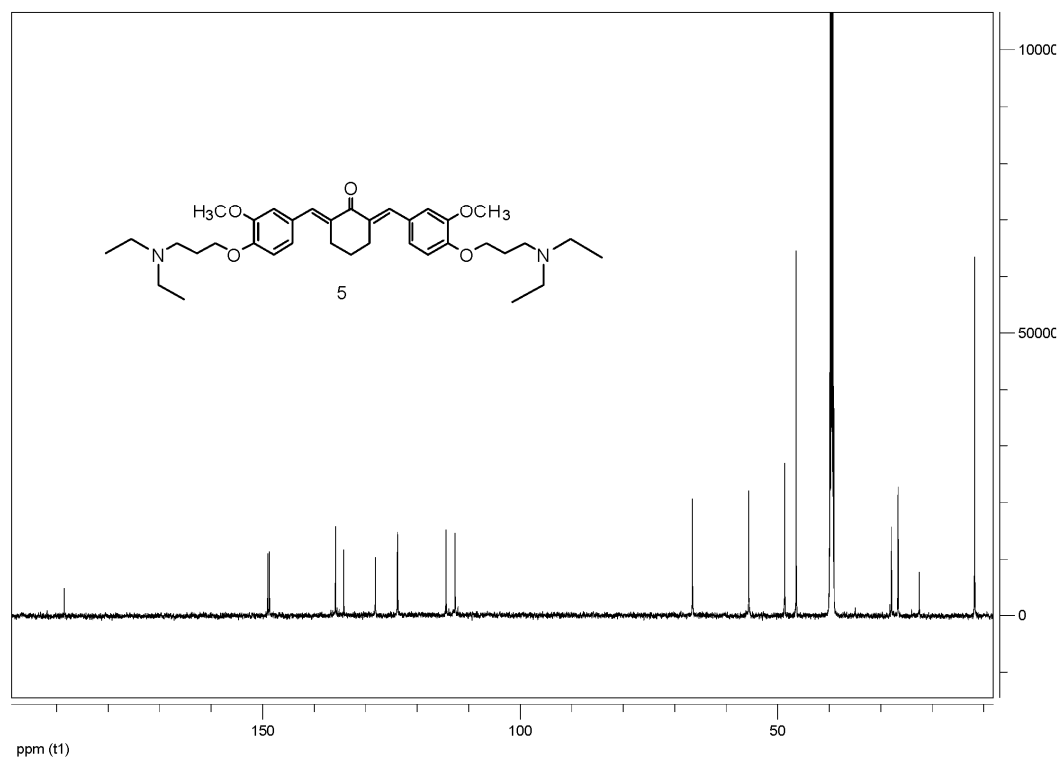


Figure S5 standard curve and solubility of compound 29

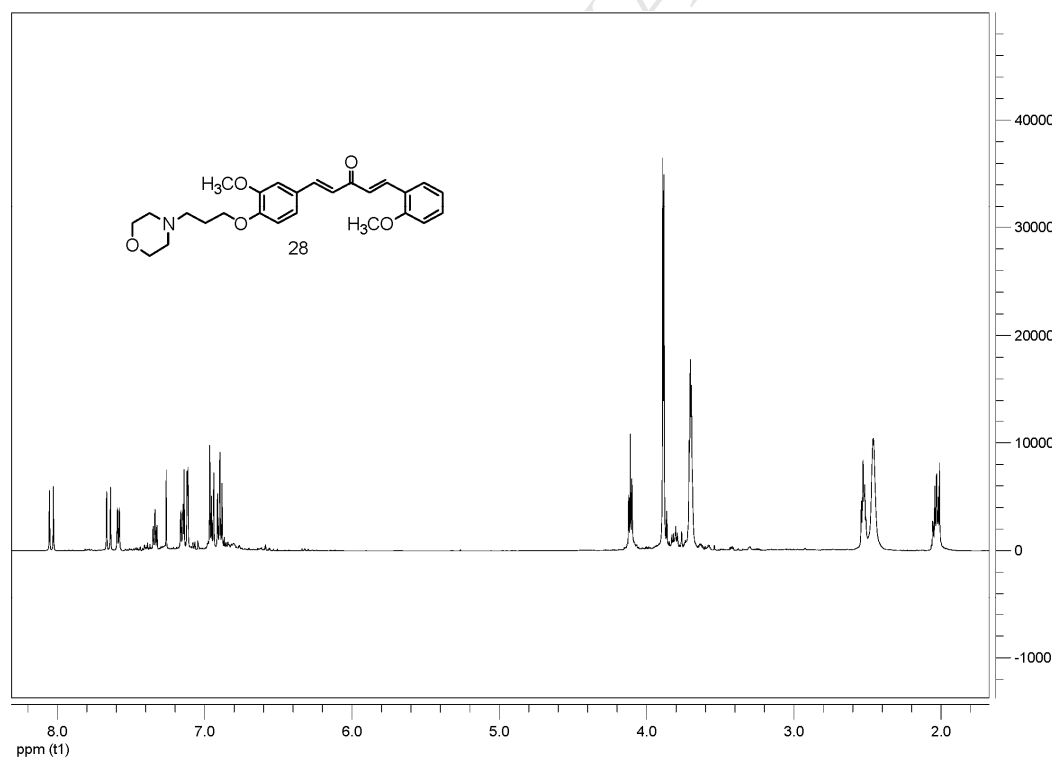
Original $^1\text{H-NMR}$ and $^{13}\text{C-NMR}$ spectra of representative compounds

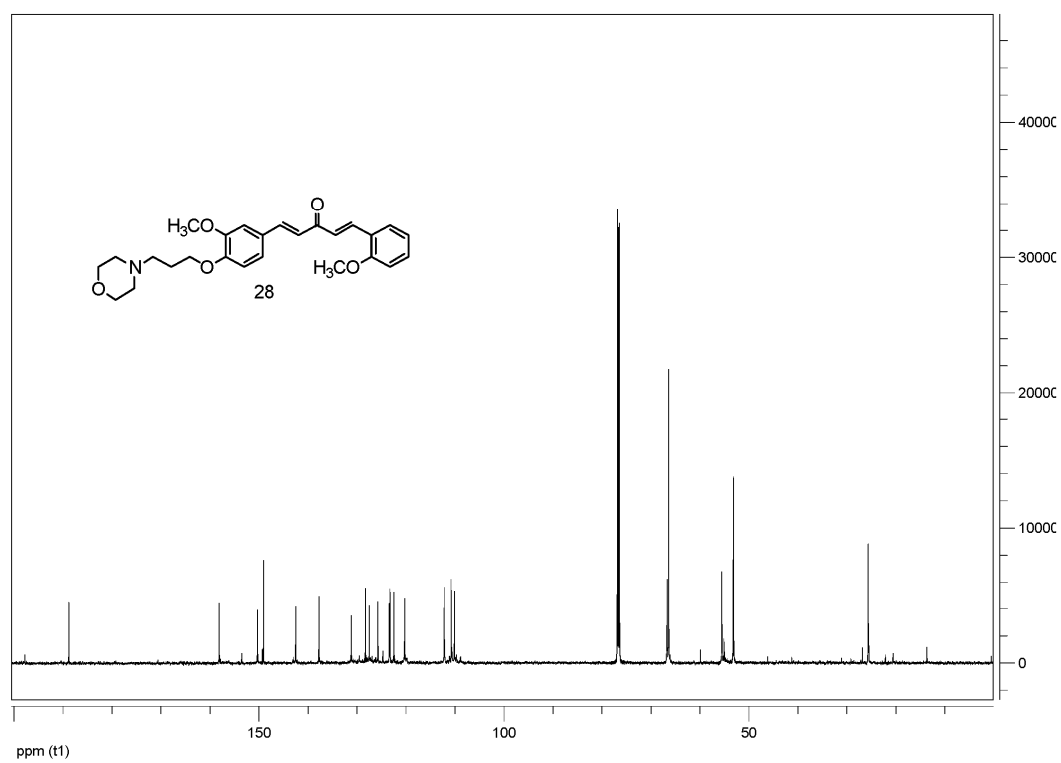
$^1\text{H-NMR}$ and $^{13}\text{C-NMR}$ original images of compound 5



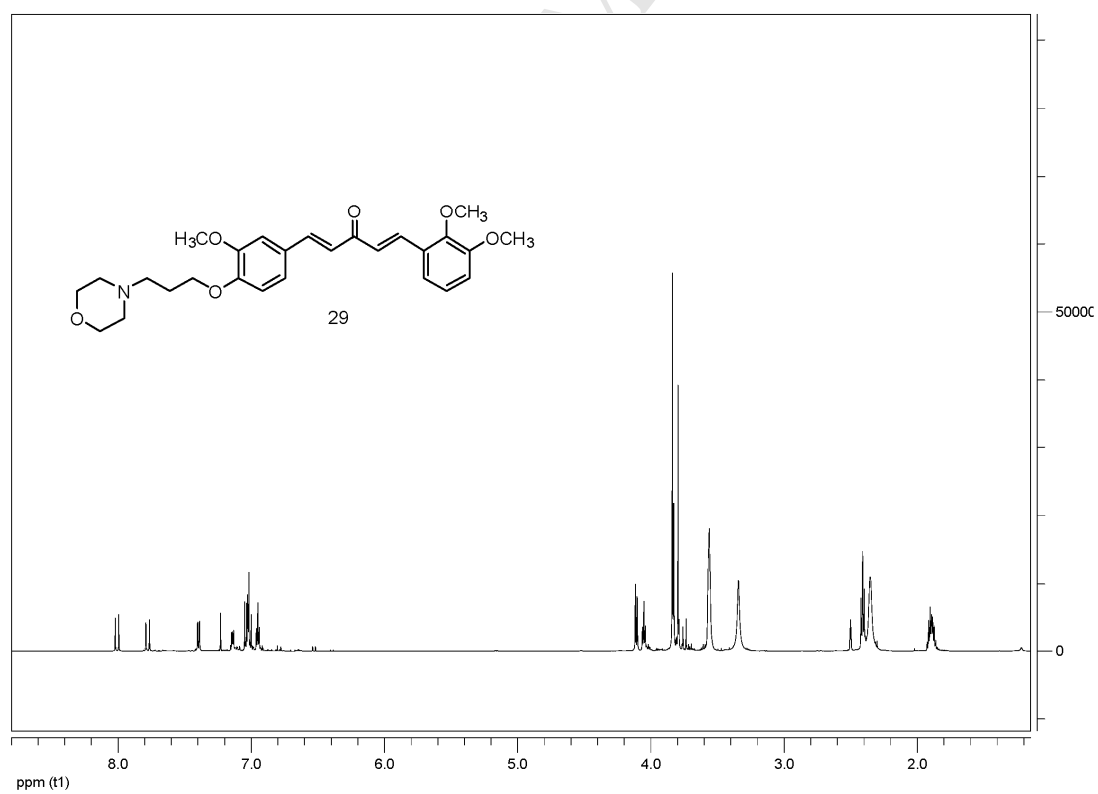


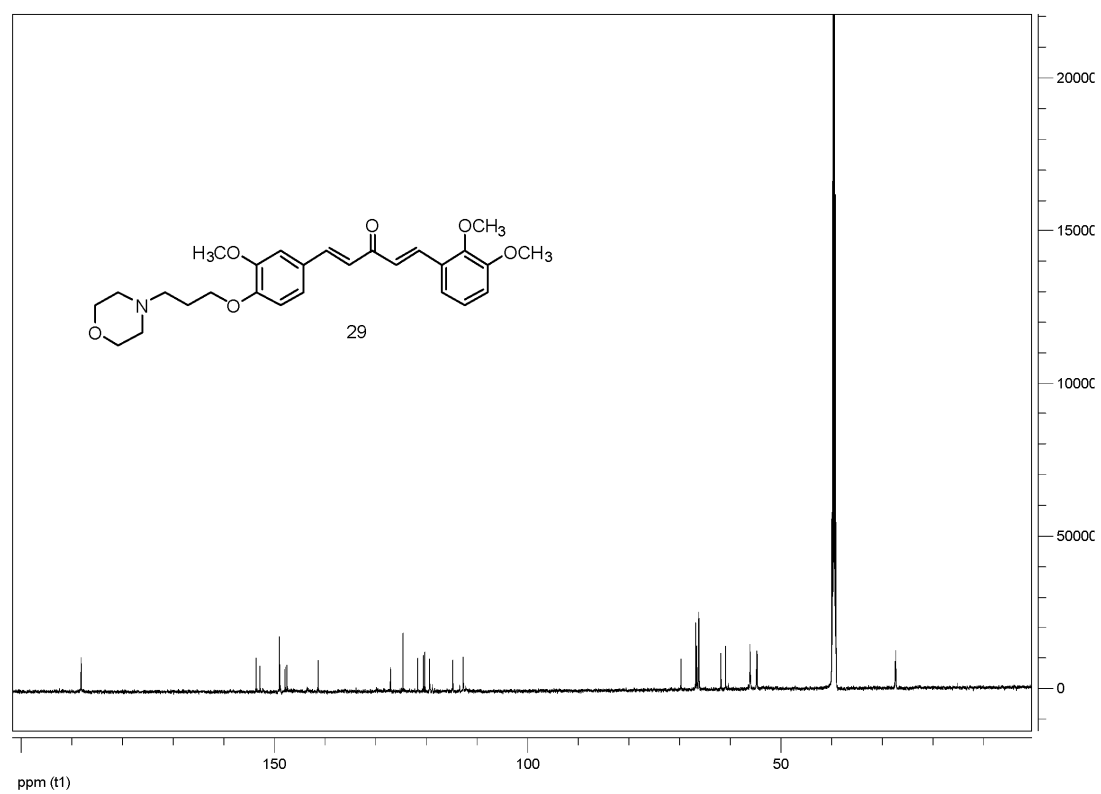
¹H-NMR and ¹³C-NMR original images of compound 28





¹H-NMR and ¹³C-NMR original images of compound 29





ACCEPTED MANUSCRIPT